Fluorescent Sterols and Cholesteryl Esters as Probes for Intracellular Cholesterol Transport

Libertas Academica
FREEDOM TO RESEARCH

Supplementary Issue: Cellular Anatomy of Lipid Traffic

Katarzyna A. Solanko*, Maciej Modzel*, Lukasz M. Solanko and Daniel Wüstner

Department of Biochemistry and Molecular Biology, University of Southern Denmark, Odense M, Denmark. *These authors contributed equally to this work.

ABSTRACT: Cholesterol transport between cellular organelles comprised vesicular trafficking and nonvesicular exchange; these processes are often studied by quantitative fluorescence microscopy. A major challenge for using this approach is producing analogs of cholesterol with suitable brightness and structural and chemical properties comparable with those of cholesterol. This review surveys currently used fluorescent sterols with respect to their behavior in model membranes, their photophysical properties, as well as their transport and metabolism in cells. In the first part, several intrinsically fluorescent sterols, such as dehydroergosterol or cholestatrienol, are discussed. These polyene sterols (P-sterols) contain three conjugated double bonds in the steroid ring system, giving them slight fluorescence in ultraviolet light. We discuss the properties of P-sterols relative to cholesterol, outline their chemical synthesis, and explain how to image them in living cells and organisms. In particular, we show that P-sterol esters inserted into low-density lipoprotein can be tracked in the fibroblasts of Niemann–Pick disease using high-resolution deconvolution microscopy. We also describe fluorophore-tagged cholesterol probes, such as BODIPY-, NBD-, Dansyl-, or Pyrene-tagged cholesterol, and eventual esters of these analogs. Finally, we survey the latest developments in the synthesis and use of alkyne cholesterol analogs to be labeled with fluorophores by click chemistry and discuss the potential of all approaches for future applications.

KEYWORDS: fluorescent sterols, sterol trafficking, optical microscopy, imaging, metabolism, endocytosis

SUPPLEMENT: Cellular Anatomy of Lipid Traffic

CITATION: Solanko et al. Fluorescent Sterols and Cholesteryl Esters as Probes for Intracellular Cholesterol Transport. *Lipid Insights* 2015:8(S1) 95–114 doi:10.4137/LPI.S31617.

TYPE: Review

RECEIVED: December 3, 2015. **RESUBMITTED:** April 4, 2016. **ACCEPTED FOR PUBLICATION:** April 7, 2016.

ACADEMIC EDITOR: Tim Levine, Editor in Chief

PEER REVIEW: Two peer reviewers contributed to the peer review report. Reviewers' reports totaled 967 words, excluding any confidential comments to the academic editor.

FUNDING: A grant from the Villum Foundation funded the salary of MM during the conduct of this study. A grant from the Novo Nordisk Foundation funded the salaries of LS and KS during the conduct of this study. The authors confirm that the funder had no influence over the study design, content of the article, or selection of this journal.

COMPETING INTERESTS: Authors disclose no potential conflicts of interest.

CORRESPONDENCE: wuestner@bmb.sdu.dk

Paper subject to independent expert single-blind peer review. All editorial decisions made by independent academic editor. Upon submission manuscript was subject to anti-plagiarism scanning. Prior to publication all authors have given signed confirmation of agreement to article publication and compliance with all applicable ethical and legal requirements, including the accuracy of author and contributor information, disclosure of competing interests and funding sources, compliance with ethical requirements relating to human and animal study participants, and compliance with any copyright requirements of third parties. This journal is a member of the Committee on Publication Ethics (COPE).

Published by Libertas Academica. Learn more about this journal.

Introduction

Cholesterol is a fundamental component of animal plasma membranes (PMs). It is also present in plant cells, but in significantly smaller amounts.[1,2] Ergosterol is the major sterol in fungi, including baker's yeast, *Saccharomyces cerevisiae*, where this sterol fulfills similar functions as cholesterol in mammalian cells. Among the major lipid species localized in membranes, sterols are chemically unique. Cholesterol exhibits very low water solubility. Therefore, it is transported in plasma as a component of lipoproteins, either in the limiting phospholipid monolayer or in an esterified form as a component of the lipoprotein core. The basic structure of cholesterol consists of four fused rings to which an alkyl chain is attached at carbon 17 in the D-ring, while a hydroxyl group is linked in β-orientation to carbon 3 in the A-ring (Fig. 1A). A single double bond is found between carbon 5 and 6 in the B-ring. The two methyl groups in the ring system point toward the β-surface (Fig. 1B). The orientation of cholesterol in lipid membranes is typically with the 3β′-hydroxy group pointing toward the interface, while the alkyl side chain is buried in the hydrophobic interior of the bilayer, and the smooth α-surface can interact with the saturated fatty acyl chains of neighboring phospholipids. The extent of cholesterol alignment parallel to the bilayer normally depends on the acyl chain saturation of the host phospholipids as well as of the cholesterol concentration in the bilayer. Polyunsaturated membranes are an exception, as cholesterol preferentially lies between the two bilayer leaflets.[3] Adding cholesterol to a membrane made of phospholipids with monounsaturated fatty acids will condense and rigidify the bilayer, and this condensing effect is instrumental for cholesterol-mediated regulation of bending stiffness, permeability to small solutes, receptor aggregation, and so on. Further information on the relationship between sterol structure, its membrane properties, and intracellular transport can be found in recent reviews.[4–6]

The majority of cholesterol is synthesized de novo; only a small fraction comes from dietary sources (Fig. 1C). Biosynthesis as well as uptake of cholesterol from plasma via circulating lipoproteins is strictly regulated. Several feedback loops ensure the exact amount of cholesterol the cells need for their physiological function. The complex metabolic control of cholesterol synthesis, uptake, and efflux has been recently reviewed in

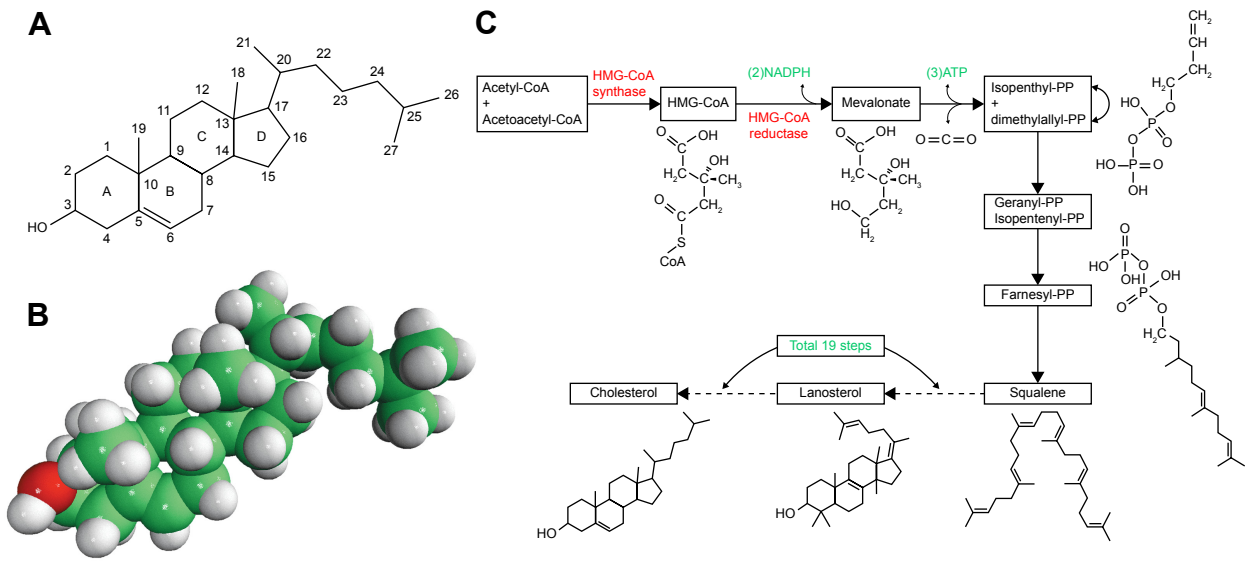

Figure 1. Structure and biosynthesis of cholesterol biosynthesis. The chemical structure with atom numbering (**A**) and a space-filling representation (**B**) (Structure shown above kindly supplied by Avanti Polar Lipids, Inc.). An overview of cholesterol's biosynthesis (**C**).

detail and will not be discussed further.[6–8] We will just emphasize that regulatory networks controlling sterol metabolism are mechanistically linked to the size of various cellular cholesterol pools, such as the endoplasmic reticulum (ER) and the PM. This underlines the importance of understanding cholesterol trafficking pathways from the aspect of metabolic control. Cholesterol is not homogenously distributed in mammalian cells. Depending on the cell type, the PM contains about 60% of the total cellular cholesterol. The ER is the organelle where most steps of synthesis of cholesterol take place, but the total sterol concentration is low when normalized to total lipids in ER membranes.[9] This is due to the fact that cholesterol is rapidly transferred from the ER to other organelles.[10] It has to be emphasized that cholesterol moves rapidly between intracellular organelles making use of vesicular trafficking and nonvesicular pathways. Accordingly, the size of cellular cholesterol pools can be rapidly adapted according to metabolic needs.

Excess cholesterol is known to have cytotoxic effects in mammalian cells, as it triggers the unfolded protein response and apoptosis in free cholesterol-loaded cells.[11] Thus, cells adapt to remove excess cholesterol in several ways: first, cholesterol efflux transporters can be upregulated via the liver X receptor (LXR) family of transcription factors. This results in the efflux of cholesterol together with phospholipids to high-density lipoprotein (HDL) and its apoprotein, apoA1. Second, a slight increase of cholesterol above the physiological set point results in blocked export of sterol response element binding protein 2 (SREBP2) from the ER to the Golgi. Herein, SREBP2 would be processed to become a transcription factor controlling the expression of cholesterol-synthesizing enzymes, such as 3-hydroxymethyl-3-methylglutaryl coenzyme A reductase (HMGR) together with the low-density lipoprotein (LDL) receptor.[12,13] Expanding cellular cholesterol levels also triggers activation of acyl-coenzyme A acyl transferase (ACAT) in the ER.[14,15] ACAT catalyzes reesterification of free cholesterol in the ER, and excess cholesteryl esters (CEs) become stored in lipid droplets (LDs).

LDL particles are the major cholesterol carriers in the blood, and high plasma concentrations of LDL are correlated with an increased risk of developing atherosclerosis and cardiovascular diseases.[16,17] After binding to its receptor in clathrin-coated pits and uptake of the LDL-receptor complex, the LDL is released from its receptor in a pH- and calcium (Ca^{2+})-dependent manner within early endosomes.[16] Degradation of LDL, including hydrolysis of its CEs by acid lipase, is proposed to take place after or during the structural and functional transition of early into late endosomes (LEs). Unrestrained cholesterol accumulation is deleterious for cells and associated with a number of diseases such as atherosclerosis and lysosomal storage disorders.[18] For example, Niemann–Pick disease type C (NPC) is a neurodegenerative disorder caused by a mutation in either protein NPC1 or protein NPC2.[19] NPC1 is a large transmembrane protein mostly located in LE/LYSs and also found in the trans-Golgi network (TGN).[19] NPC2 is a small protein found mainly in lysosomes and LEs, which binds cholesterol and presumably hands it off to NPC1. The proteins seem to bind the opposite sides of a cholesterol molecule.[20] Loss of function in either NPC1 or NPC2 has been shown to cause severe lysosomal accumulation of cholesterol, glycosphingolipids, sphingosine, and sphingomyelin.[19,21] Fibroblasts lacking functional NPC1 or NPC2 hydrolyze LDL-derived CEs normally, but have a strongly reduced ability to elicit normal regulatory responses.[22,23] Both NPC1 and NPC2 bind cholesterol and intrinsically fluorescent cholesterol analogs, such as dehydroergosterol (DHE) and cholestatrienol (CTL).[6] It is generally assumed that these proteins specifically control the transport

of LDL-derived sterols out of LEs.[24,25] One model proposes that NPC2 binds cholesterol after hydrolysis of LDL CEs in the lumen and transfers it to NPC1 for export from LEs to various target organelles including the ER and the PM.[25] In vitro experiments demonstrated that NPC2 accelerates sterol exchange between membranes several-fold, and this process is further enhanced under conditions found in acidic endosomal compartments.[24,26] A mechanistic link between NPC2s in in vitro and in vivo functions is missing.[27] A summary of cholesterol transport through the endocytic pathways is shown in Figure 2. Further discussion of proteins being involved in endosomal cholesterol transport as well as of the proposed underlying mechanisms can be found elsewhere.[6]

Fluorescent Probes for Cholesterol Studies in Cells

Fluorescence microscopy is one of the few methods that can provide information on the distribution and dynamics of molecules in living cells. However, as cholesterol and its physiological esters are not fluorescent, for imaging by this technique, their fluorescent analogs must be employed. The main challenge here is to find analogs that, while being fluorescent, would introduce minimal changes to the structure and properties (and thus distribution and transport pathways) of cholesterol or CEs. An alternative approach is to use cholesterol-binding and fluorescent molecules. Herein, one can either use certain bacterial toxins, such as perifringolysin O (PFO). For imaging, PFO can be linked to a fluorescent dye or expressed as fluorescent protein-tagged construct in cells, or one can apply intrinsically fluorescent polyene antibiotics, such as filipin or nystatin.[28,29] Filipin binds sterols with a free 3′-hydroxy group and is, therefore, often used to determine total cholesterol distribution by microscopy.[30] Filipin and PFO derivatives work well in fixed cells and have been used in high-content screening assays or in ultrastructural studies using electron microscopy (see Table 1).[31–35] However, such probes do not allow one to study inter-organelle

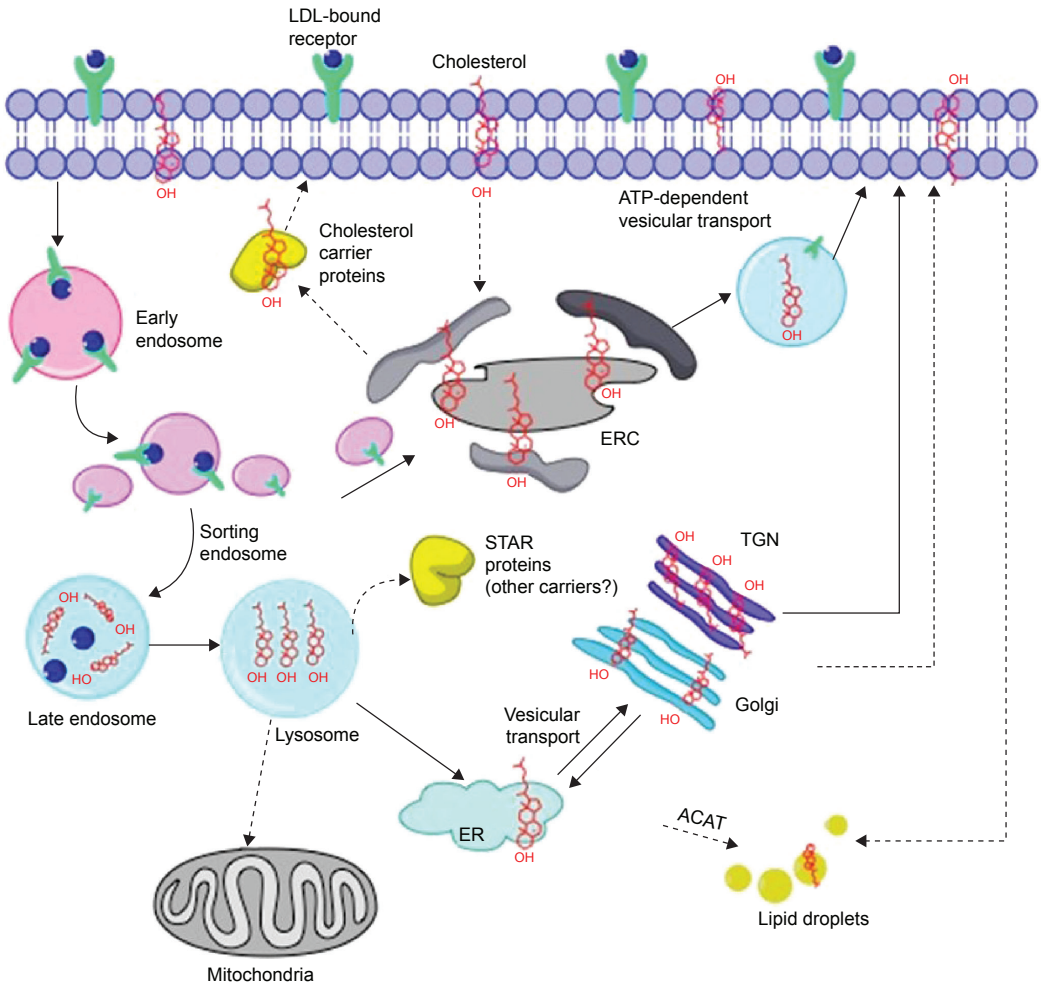

Figure 2. Schematic illustration of cholesterol transport. Cholesterol uptake via LDL particles, its liberation in late endosomes and lysosomes (LE/LYSs), and trafficking from the PM to the endocytic recycling compartment (ERC), the TGN, the ER, or to mitochondria, as happening in steroidogenic cells, is shown. Between these membranes, cholesterol moves by vesicular (lined arrows) and/or nonvesicular pathways (dashed arrows). See the text for more details. Adapted from Wüstner D, Solanko LM and Lund FW. 2012. Cholesterol trafficking and distribution between cellular membranes., in: I.a.B. Levitan F. (Ed.) Cholesterol regulation of ion channels and receptors., John Wiley & Sons Inc., pp. 3–25.

Table 1. Commonly used fluorescent sterol probes; typical applications, advantages and drawbacks.

CHOLESTEROL PROBE	APPLICATION	PROS	CONS
Fluorophore bound to bacterial toxins as perifringolysin O	Screening assays Assessment of transbilayer sterol distribution Can be combined with electron microscopy	Used to assess threshold concentrations of cholesterol in model & cell membranes Partly useful for super-resolution microscopy	Cannot track inter-organelle transport nor sterol diffusion, do not bind esters Trafficking studies only in fixed cells, unless genetically encoded
Intrinsically fluorescent (polyene) antibiotics, as filipin	Screening assays Phenotyping of lysosomal storage disorders Can be combined with electron microscopy	Reliable quantitative measure of cholesterol Partition into lo phase in model membranes Useful for assessing cholesterol content in tissue samples	Cannot track inter-organelle transport or be used in living cells, do not bind esters Requires UV optics Cross-reactivity to gangliosides
DHE (esters)	Trafficking studies in mammalian cells, yeast and nematodes Membrane biophysics (Lipoprotein structure, dynamics, transport & metabolism)	Closest analogue to ergosterol followed by cholesterol; gets bound and transferred by STPs Induces and partitions into lo phase in model membranes Can replace cholesterol or ergosterol in sterol-auxotroph organisms	Low brightness, requires UV optics, bleached easily, limited substrate for ACAT1 in mammalian cells
CTL (esters)	Trafficking studies Membrane biophysics (Lipoprotein structure, dynamics & metabolism) Lead structure for fluorescent oxysterols	Closest analogue of cholesterol; gets bound and transferred by STPs Partitions into lo phase in model membranes & orders phospholipids almost as good as cholesterol	Low brightness, requires UV optics, bleached easily
Parinaric acid cholesteryl esters	Probing membrane and lipoprotein structures	Does not alter sterol structure	Cannot track cholesterol after hydrolysis Requires UV optics
BODIPY-cholesterol (esters)	Versatile, used in many kinds of studies including trafficking in mammalian cells & In vivo imaging (zebrafish) Screening assays (for cholesterol efflux) Membrane biophysics	High brightness and good photostability Partitions into lo phase in model membranes Ease of use in conventional fluorescence microscopy Partly useful for dynamic super-resolution microscopy	High affinity to lipid droplets, thereby partial miss-targeting in cells No ordering of fatty acyl chains in model membranes Usability in yeast is questionable Not substrate for all known STPs
Dansyl-cholesterol	Trafficking studies ACAT activity in living cells	High brightness, small molecule Ease of use in conventional fluorescence microscopy	Partitions into ld phase in model membranes Prone to bleaching Not substrate for all known STPs
NBD-cholesterol (esters)	Monitoring physical properties of membranes Trafficking studies ACAT activity in living cells	Easily absorbed from media Ease of use in conventional fluorescence microscopy	Prone to bleaching, orientation in membranes opposite to cholesterol Partitions into ld phase in model membranes Not substrate for all known STPs
Pyrene-cholesterol	Studying exchange between lipoproteins Transport in cells	Forms excimers with potential use in membrane sterol agrgegation	No esterification Requires UV optics Partition preference and binding to STPs not known
Dye-linked PEG-cholesterol (e.g. KK114-PEG-Chol)	Tracking of cholesterol in PM (i.e. lateral diffusion in living cells)	Very photostable Very useful for dynamic super-resolution microscopy	No fip-flop & no non-vesicular transport No metabolism
Click chemistry substrates	Versatile, e.g. enzymatic assays, trafficking studies Analogues of cholesterol and of oxysterols	Mimic cholesterol very well before click reaction, many possible analytical enhancers to optimize fluorescence Useful for super-resolution microscopy	Cannot be used in living cells (i.e. after the click reaction) Behaviour of fluorescent analogue after click reaction is poorly characterized

sterol transport dynamics, and with the exception of fluorescent protein-linked fringolysin, variants cannot be applied to living cells. Filipin perturbs membrane structure and has even been shown to bind gangliosides in addition to cholesterol.[36–39] Most importantly, neither filipin nor PFO and related toxins detect sterol esters, and such probes do not allow for discriminating endogenously synthesized from exogenous cholesterol taken up from circulating lipoproteins, like LDL. Thus, for specific and reliable tracking of the LDL cholesterol pathway in living cells, fluorescent analogs of CEs are needed, and developing suitable sterol esters is an important but a challenging task.

Fluorescent analogs of cholesterol and its esters can be discriminated into intrinsically fluorescent sterols and extrinsic or tagged sterol probes. Intrinsically fluorescent sterols contain several conjugated double bonds as an intrinsic part of the molecule, either in the steroid ring system or in the fatty acyl moiety in the case of an ester. Extrinsically fluorescent sterol probes have a label moiety attached to either the steroid backbone or the fatty acyl chain in the case of a CE analog. The very first attempt of using intrinsic fluorescence was by introducing conjugated double bonds into the A-ring of cholesterol creating sterophenol or by employing aromatic steroid hormones such as estradiol or estrogen derivatives such as dihydroequilenin.[40,41] Sterols with an aromatic A-ring have excitation around 285 nm and a slight emission centered around 308 nm.[40,42] Using iodide as collisional quencher, sterophenol was used to determine the transbilayer dynamics of a cholesterol probe.[40] However, it turned out that a completely planar A-ring found in aromatic sterol probes is not compatible with the properties of cholesterol, as comprehensively reviewed by Schroeder more than 30 years ago.[42] Equilenin and dihydroequilenin contain a larger conjugated system involving the A- and B-rings of the sterol backbone and show excited state deprotonation reactions of the 3-hydroxy group.[41] Thus, these probes are of interest in the studies on steroid hormones but very different from cholesterol. Since the conjugated double bonds of most intrinsically fluorescent sterols resemble the basic structure of polyenes, they are also called polyene sterols (P-sterols). Such P-sterols extend the conjugated system based on the double bond of the cholesterol in the B-ring, as exemplified for DHE and CTL below. These P-sterols do not have completely planar rings in the steroid backbone.

Intrinsically Fluorescent Cholesterol (Ester) Analogs

Dehydroergosterol. DHE is the P-sterol that is most widely used in cholesterol trafficking research. DHE is a direct derivative of ergosterol, from which it differs only in having one additional double bond in the ring system (compare Fig. 3A and B). The resulting conjugated system of three double bonds makes DHE slightly fluorescent in the ultraviolet (UV) range. DHE is a sterol naturally occurring in yeast cells, for example, *S. cerevisiae*, and other fungi.[43] *Penicillium candidum*, a fungus used for the production of camembert, synthesizes DHE, and this sterol—but not ergosterol—has been shown to be the active dietary compound of these organisms for protecting

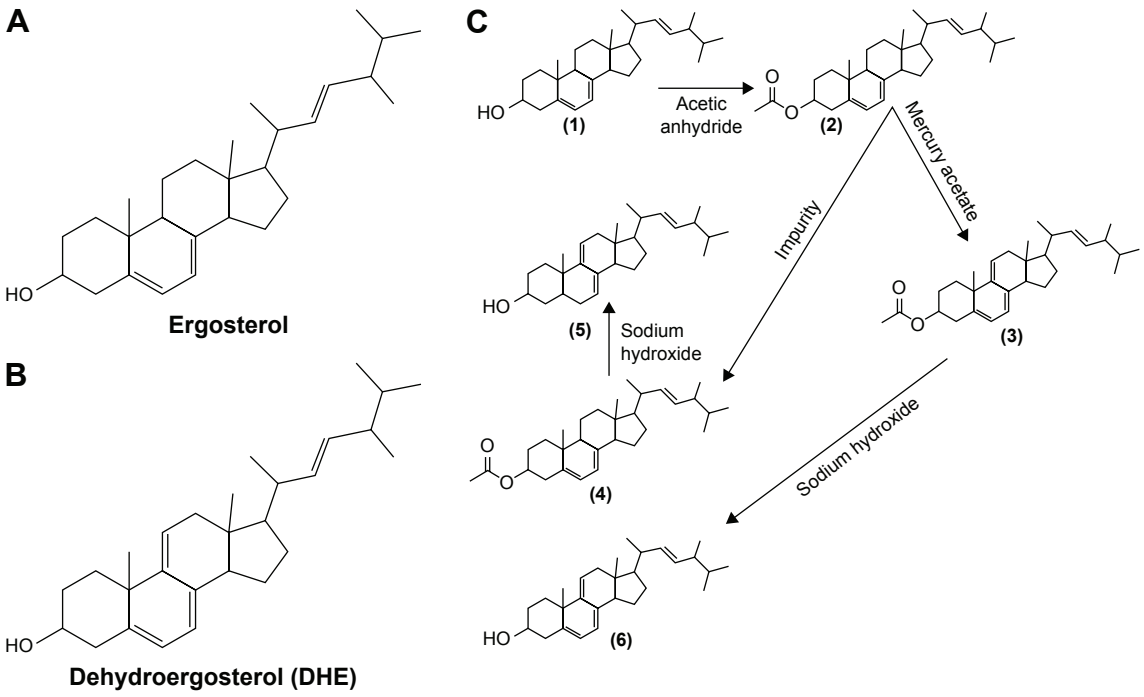

Figure 3. Schematic pathway of DHE synthesis and possible side pathways. The chemical structure of ergosterol (**A**) and that of DHE having only one additional double located in the C-ring (**B**). (**C**) Synthesis of DHE from ergosterol and the possible side reactions leading to impurities: (**1**) ergosterol; (**2**) ergosteryl acetate; (**3**) dehydroergosteryl acetate; (**4**) ergosteryl D acetate; (**5**) ergosterol D; and (**6**) DHE. Adapted from Ref. 43.

microglia cells in culture.[44] This suggests a novel approach for using DHE as a dairy additive for preventing microglia inflammation and onset of dementia.[44] While DHE is commercially available, it usually contains a significant amount of impurities. This is detrimental to analysis by imaging, as the impurities can compete with DHE itself, or have other effects, including cytotoxicity.[45] For synthesis of DHE (Fig. 3C), ergosterol is first converted into an ester form (ergosteryl acetate) in the reaction with acetic anhydride. This procedure is necessary in order to protect the 3′OH group during the subsequent oxidation by mercury (II) acetate ($(CH_3COO)_2Hg$) and acetic acid (CH_3COOH). The reaction is carried out in boiling ethanol for two hours. Subsequently, the reaction mixture is cooled down and the solvent is evaporated under reduced pressure in a rotary evaporator. A crude solid is dissolved in dichloromethane or tetrachloromethane (CCl_4) and purified using water extraction (with the addition of sodium hydroxide to hydrolyze the ester). Mercury(II) acetate is highly soluble in water, and its leftovers are usually removed together with the water fraction. We typically purify DHE synthesized from ergosterol by washing the organic layer several times with water, drying with anhydrous $MgSO_4$, and then applying active carbon (for example Norit®). The solvent is evaporated in vacuum, and the product is crystallized from 1:1 acetone:ethanol mixture at –20°C. The crystalline product is gently washed in a last step with ice-cold petroleum ether. The final product is kept in the dark and under nitrogen until use. By this procedure, we typically reach a reaction yield of 60%–70% and a stable product for several months.

DHE is the closest analog of ergosterol from which it differs only by having one additional double bond in the ring system. Accordingly, it can be used by the yeast *S. cerevisiae* as the only sterol source, when growing under anaerobic conditions.[46,47] It can also be used as sterol source by mammalian cells being partly sterol auxotroph.[43] DHE is esterified in yeast as ergosterol, and its cellular uptake requires the activity of ARE2, the yeast homolog of ACAT.[46,47] In mammalian cells, DHE is esterified when taken up by nonlipoprotein pathways, though the esterification is slightly lower than that of cholesterol (Refs. 48 and 49 and our unpublished observations). In in vitro experiments, DHE was a poor substrate and less-efficient allosteric activator of ACAT1 compared with cholesterol.[50] This can at least partly explain its less-effective esterification in mammalian cells. DHE cannot activate processing of SCAP/SREBP2 as cholesterol does, suggesting that it fails to bind to several cholesterol metabolizing proteins in the ER membrane.[51] Such shortcomings must be considered when using DHE in studies on cholesterol metabolism in mammalian cells. For studies on sterol trafficking and metabolism in yeast, DHE can be used without concerns, as DHE is the closest possible fluorescent analog of ergosterol.

DHE has also been used for decades for spectroscopic studies of cholesterol distribution in membranes.[42] Recent experimental and computational biophysical studies have complemented such earlier investigations by showing that DHE mimics cholesterol well at moderate concentrations in membranes of up to 10 mol%.[52,53] Above that concentration, the ability of DHE to order phospholipid acyl chains ceases, which is different from cholesterol.[53] However, DHE mimics ergosterol well in this respect, as ergosterol also condenses and rigidifies monounsaturated phospholipid membranes only up to 10 mol% in a linear concentration dependence.[54,55] This is also the upper limit of the typical amount of DHE required in cellular membranes in live-cell imaging applications.[56] By combining electronic structure calculations with time-resolved fluorescence studies, it was shown that DHE's transition dipole is parallel to the long axis of the molecule.[52] Having this information, one can conclude about sterol organization in the membrane from (time-resolved) fluorescence polarization spectroscopy. In the majority of isotropic solvents, DHE exhibits a fluorescence lifetime of approximately 0.3 nsec.[57] In membranes made of 1-palmitoyl-2-oleyl-phosphatidylcholine (POPC), its lifetime is around 0.8 nsec and only slightly dependent on sterol concentration in the membrane.[2,52,57] These properties together with the nearly linear relationship between emission intensity and mole fraction of DHE in bilayers[52] make this P-sterol a quantitative probe of cholesterol concentration in models and cell membranes. Anisotropic emission of DHE is slightly concentration dependent in model membranes.[2,52,58] This has been suggested to be a consequence of transbilayer dimer formation of DHE similar to that proposed for cholesterol at low concentrations.[58,59] Maximum fluorescence emission of DHE is around 373 nm in POPC membranes, with two shoulders at 395 and 355 nm, respectively. Since quantum chemical calculations find only one transition for DHE from the singlet ground to the excited state, the two shoulder peaks are likely a consequence of vibrational coupling.[52] A low extinction coefficient ($\varepsilon \approx 11{,}000\ M^{-1}\ cm^{-1}$) and quantum yield ($\Phi_f = 0.04$ in ethanol) for DHE results in low molecular brightness (ie, the product of ε and Φ_f). This requires UV-optimized optics combined with highly sensitive CCD detectors for imaging DHE in living cells.[60] Alternatively, DHE can be imaged by three-photon excitation, as shown in mammalian cells and in living nematodes.[61–63] Advantages of this technique are its intrinsic sectioning capability and its deeper penetration into the specimen due to a lower scattering of the infrared laser excitation compared with single-photon excitation.[64] Since the excitation spot is confined to a thin axial region of about 600–800 nm within the specimen, any photobleaching is confined to just the slice actually recorded. This is particularly useful for 3D imaging of DHE in cells and animals (Fig. 4). However, the advantages are somehow balanced by the low intensity of DHE images obtainable by multiphoton excitation microscopy.[62] The image quality can be significantly improved by averaging several frames for getting one image with good signal-to-noise ratio.[62] This is exemplified in Figure 4A and B, where a polarized hepatoma

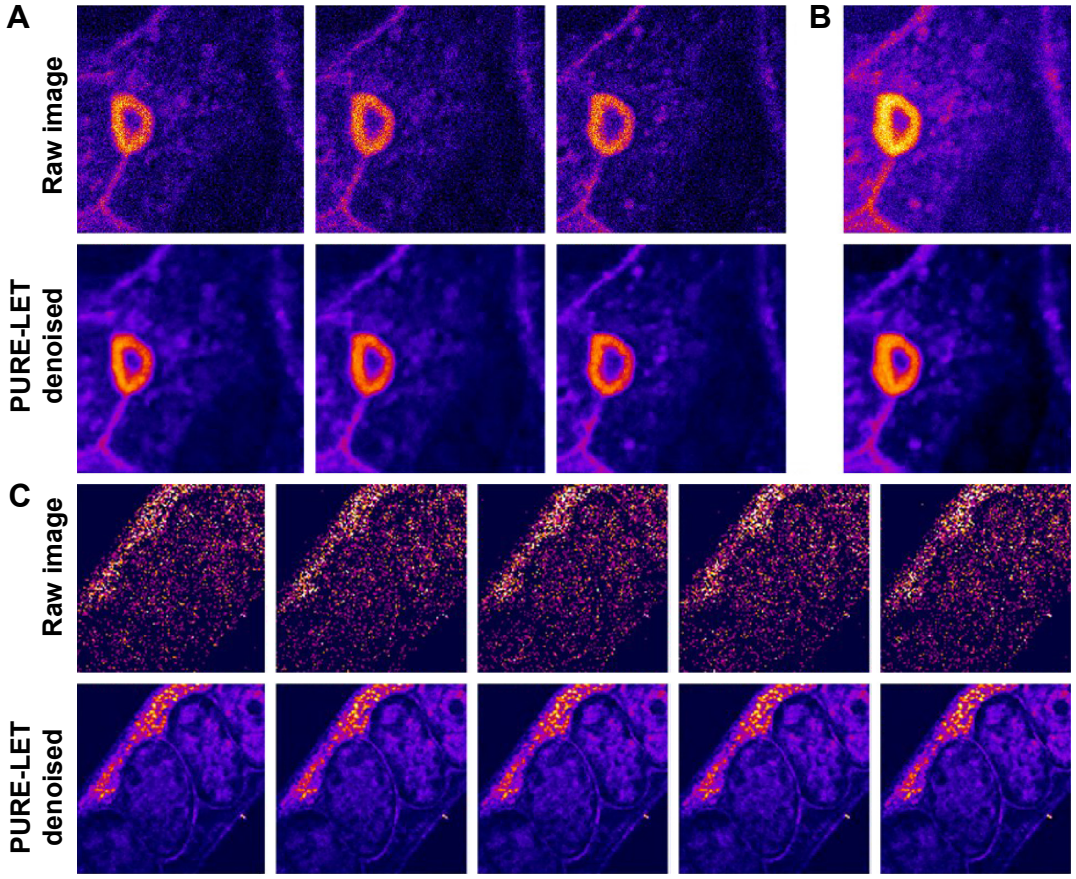

Figure 4. Three-photon imaging and PURE-LET image denoising for visualization of DHE in polarized HepG2 cells and in nematodes. A, B, HepG2 cells were labeled for 2 minutes with DHE from a DHE/cyclodextrin complex, washed and chased for 30 minutes at 37°C. A field with polarized cells forming an intercellular BC was selected and imaged on a home-built multiphoton microscope using a femtosecond-pulsed Ti:Sapphire laser emitting at 930 nm as excitation source. (**A**) Selected intensity-averaged frames acquired along the optical axis and (**B**) corresponding maximum intensity projection of all six intensity-averaged images from 10 acquisitions each, either prior to (upper panels) or after PURE-LET denoising (lower panels). (**C**, upper row) Adult glo-mutant nematodes grown on agar plates containing DHE and imaged on the same system and (**C**, lower row) result after PURE-LET denoising. Images are shown color-coded with a FIRE-LUT. See text and Refs. 62, 63, and 188 for further details.

HepG2 cell couplet labeled with DHE for two minutes and 10 frames were averaged for at each *z*-position. In this way, we can obtain good-quality images with clear visualization of the central biliary canaliculus (BC), and subapical accumulation of sterol-rich vesicles (Fig. 4A and B; only every second acquired image is shown). Further improvement is possible by a statistical method called image denoising, as shown in the lower panels of Figure 4A and B.[65] However, UV-sensitive wide field imaging is much easier and faster than multiphoton imaging of DHE in cells. In an attempt to track sterol dynamics in living nematodes, we faced the problem of strong intestinal autofluorescence in these animals.[66] To overcome this problem, we developed bleach-rate-based image segmentation, making use of the much faster photobleaching of DHE compared with autofluorescence.[63,67] This approach is very efficient in discriminating DHE from autofluorescence and also works in other applications.[46] Importantly, DHE has a significant quantum yield (0.09) for photosensitization of singlet oxygen and seems to be the major photochemically active compound in some earthworm species.[68] A self-perpetuating mechanism has been postulated in which prolonged UV irradiation causes conversion of ergosterol into DHE with parallel production of singlet oxygen that further reacts with ergosterol to form ergosterol hydroperoxide. Together with other reaction products, the ergosterol hydroperoxide can convert back to DHE to be available for another round of photoreaction.[68] It must be noted, though, that UV irradiation was performed for more than 30 minutes in that study, which is much longer than the time used by us for bleach-rate imaging of DHE in nematodes. To overcome the challenge of out-of-focus blurring observed in thick specimen, three-photon excitation microscopy is superior, as it allows one to acquire thin sections in living nematodes, if they lack the majority of strongly autofluorescent gut granules (Fig. 4C). Again, PURE-LET denoising dramatically improved image fidelity and signal-to-noise ratio of such multiphoton sections (lower panel in Fig. 4C). However, only some fluorescence on the ventral site and within the eggs in such *glo*-mutant animals actually originates from DHE, the remaining being autofluorescence, connective tissue, and egg shell material, as verified

in nonstained nematodes (data not shown).[63] Thus, even though both approaches can be applied, the pros and cons of both imaging modalities must be carefully considered when imaging P-sterols such as DHE in animals or tissues.

Cholestatrienol. Structurally, CTL (Fig. 5A) is the closest fluorescent derivative of cholesterol. Similar to DHE, it contains two additional double bonds in the ring system, while the aliphatic side chain is identical to cholesterol. The first synthesis of CTL was described by Windaus et al in 1939. The molecule can be obtained from 7-dehydrocholesterol by dehydrogenation with mercury acetate in a reaction very similar to that used for transforming ergosterol into DHE (see above).[69,70] The first synthetic protocols for CTL involved purification by recrystallization, but the purified species was unstable and decomposed rapidly. When reversed-phase high-performance liquid chromatography (RP-HPLC) was used for purification instead of recrystallization (ie, a C18 RP-HPLC column and 95:5 v:v methanol:hexane mixture as the eluent), the purified product was stable at –70°C.[71] CTL can be synthesized in an analogous manner to DHE, and it remains stable in its solid form at –20°C for up to two months (our unpublished observation). Fluorescence properties and bleaching propensities of CTL are comparable with those of DHE.[72,73] However, CTL is a closer mimic of cholesterol's properties in membranes, as it shows a linear relationship between ordering capacity for fatty acyl chains and its concentration in POPC bilayers, exactly like cholesterol, but in contrast to DHE and ergosterol.[53,54,74] One of the first studies pioneered by Schroeder et al used CTL to gather information about micellar structures of sterols and to learn about sterol–protein interactions using the sterol carrier protein 2 (SCP2).[42,75] CTL was later used as the closest fluorescent cholesterol analog in many spectroscopic studies, where it was found to resemble native and deuterated cholesterol very well, for example in nuclear magnetic resonance (NMR) spectroscopy and other techniques.[53,76–78] The close similarity of CTL and cholesterol with respect to structural and dynamical properties in lipid bilayers was confirmed by molecular dynamics simulations.[79,80] Electronic structure calculations additionally indicated that the photophysical properties of CTL and DHE, such as oscillator strength and transition dipole orientation, are comparable, which further validates their similar properties in many spectroscopic studies.[2,57,76,80,81] Chong and Thompson suggested lateral segregation as a potential explanation for their observation of homotransfer for DHE and CTL in POPC membranes above critical concentrations and for the thermal-phase behavior of DHE in lipid bilayers.[82] A little later, Chong determined intensity dips of DHE at fixed stoichiometric ratios with phospholipids in the membrane and interpreted the findings using the superlattice model of membrane organizations.[83] Cholesterol is known to induce liquid ordered (lo)/liquid disordered (ld) phase coexistence in lipid membranes made of a saturated and an unsaturated phospho- or sphingolipid at high sterol mole fraction.[84,85] Since the lo phase is highly enriched in cholesterol compared with the ld phase, preferred partitioning into the lo phase is an important criterion that a good cholesterol analog must meet. For fluorescent cholesterol analogs, partitioning preference can be easily assessed by fluorescence microscopy of giant unilamellar vesicles (GUVs)[86–88] or by spectroscopic quenching studies together with a known reference marker of either the lo or the ld phase.[89,90] Unfortunately, only for

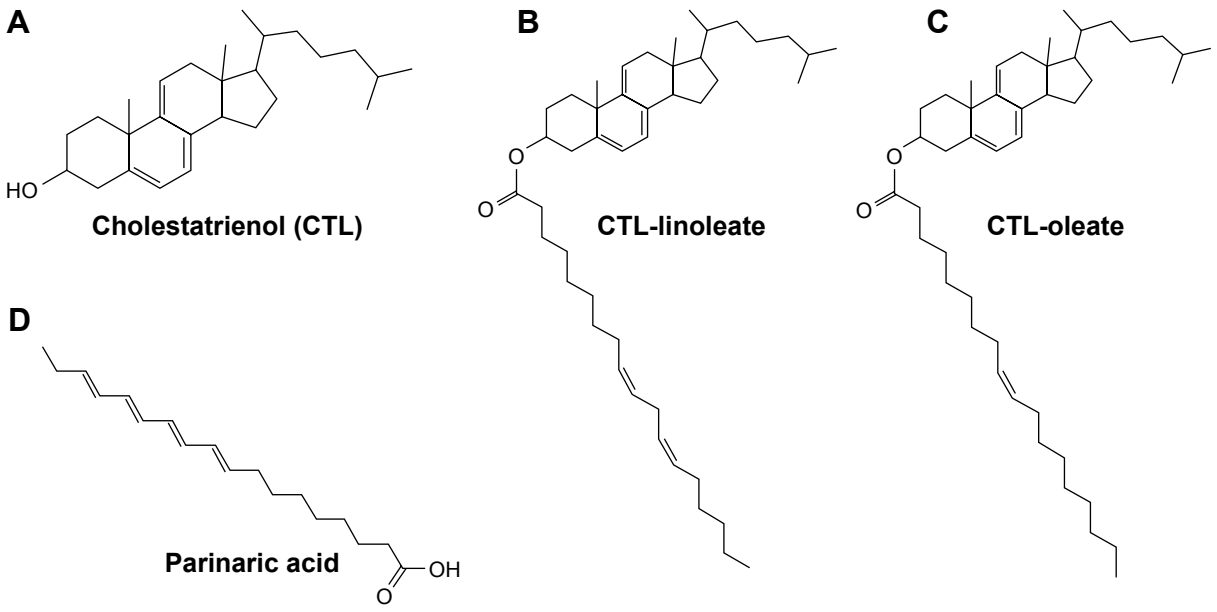

Figure 5. CTL and its esters. (**A**) The chemical structure of CTL differing from cholesterol only in having two additional double bonds that are located in the B- and C-rings, respectively. (**B**) CTL-linoleate and (**C**) CTL-oleate. (**D**) Parinaric acid is an intrinsically fluorescent polyunsaturated fatty acid, which has been esterified to cholesterol as a sensor of lipoprotein structure. See text for details and references.

few cholesterol analogs, partitioning between lo and ld phases has been reported. P-sterols such as DHE and CTL show the highest enrichment in the lo phase (ie, at least fivefold compared with the ld phase).[74,86,88] DHE was shown to be even able to induce the lo phase when substituted for cholesterol in the lipid mixture.[74] We found micrometer-sized domains in lo/ld phase-separated GUVs for DHE and demonstrated that DHE can induce liquid immiscibility in phospholipid membranes.[74] So, the existence of regular sterol arrangements and sterol domains in model membranes has been well established in several studies. In the PM of living cells, both CTL and DHE are homogeneously distributed laterally with no evidence for sterol clustering or domain formation.[72,91] Apparent local lateral enrichment is a consequence of the rough surface topography of mammalian cells and not related to the phase preference of the P-sterols in model membranes, even after cholesterol loading of cells.[72,91–94] We are not aware of any piece of experimental evidence for lateral sterol domains in the PM of intact living cells. Most evidence is extrapolated from model membrane studies, is indirect, or is only obtained after heavy experimental manipulation of the cell membranes. For example, lo-like domains can be induced from cell membranes only after detergent extraction or when treating cells with chemicals, as a combination of dithiothreitol (DTT) and paraformaldehyde (PFA).[95–98] Partitioning of fluorescent analogs of cholesterol into such lo-like domains can complement partition experiments of cholesterol probes between lo and ld phase in GUVs, as described above and elsewhere.[97,98] However, the harsh experimental manipulation makes it unlikely that such domains have precursors in the intact PM of living cells before the treatment. Indeed, inducing PM blebs at physiological temperature, in the absence of DTT or PFA, by disrupting subcortical actin using cytochalasin or after cholesterol loading did not induce phase separation of DHE.[91,92] Based on such results and many other studies, we strongly question the concept of lipid rafts, ie, the existence of lateral lipid-based domains formed due to preferred interaction of cholesterol with sphingolipids in cellular membranes. Both P-sterols are slightly enriched in the inner leaflet compared with the outer one, as assessed in quenching studies directly under the microscope.[73,99] This is again contradicting the raft concept, as sphingolipids, the proposed *raft partners* of cholesterol, reside mostly in the outer leaflet of the PM. Use of P-sterols and other fluorescent analogs of cholesterol for studying the lateral and transverse bilayer organization and dynamics of cholesterol in the PM of living cells has been recently reviewed in detail.[100] CTL is the preferred P-sterol in trafficking studies in mammalian cells and also for mechanistic studies on mammalian sterol transfer proteins.[51,73,101–103] Very recently, the synthesis of a side-chain hydroxylated derivative of CTL has been reported and applied for characterizing transport and metabolism of 25-hydroxycholesterol.[104] This 25-hydroxy-CTL is imported into cells by LDL-mediated endocytic uptake and modulates sterol homeostatic responses in a manner similar to 25-hydroxycholesterol. This confirms that P-sterols mimic their natural counterparts very closely, making them very good probes for the analysis of sterol metabolism and transport.

Cholestatrienol esters and cholesteryl parinaric acid as lipoprotein probes. CTL can be converted into ester with, for example, linoleate or oleate fatty acyl (Fig. 5B and C). Two major methods, both requiring the presence of a catalytic amount of 4-dimethylaminopyridine can be used here: a reaction with an excess of the fatty acid anhydride, or a reaction with the fatty acid and a coupling reagent, for example, dicyclohexylcarbodiimide.[105] Alternatively, the reaction can be conducted in the presence of catalytic amounts of d-block metal salts at the boiling point of water using a Dean-Stark apparatus. CTL esters can be introduced into LDL and other lipoproteins by two methods: (1) using sterol exchange proteins, such as those found in human blood plasma, which catalyze the exchange of sterol esters[106] or (2) by heptane extraction of CEs from the lipoprotein and reconstituting the core with CTL-oleate.[107] While the first method is useful for incorporating sterol ester probes into HDL, the second technique is most suitable for LDL. The first bioanalytical application of free and esterified CTL we are aware of was a spectroscopic analysis of sterol distribution in LDL and HDL.[108] In that study, CTL was shown to quench tryptophan fluorescence of the apoproteins within LDL and HDL efficiently, while the ester form, CTL-oleate (Fig. 5C) was a less efficient quencher.[108] From that, it was concluded that CEs reside in the core while cholesterol locates mostly to the phospholipid monolayer of lipoproteins. This conclusion was later confirmed in many experimental and computational studies.[108,109] A little later, CTL was used to explore the surface properties of very low-density lipoprotein (VLDL).[110] Circular dichroism, lifetime measurements, and accessibility to aqueous quenchers were used to analyze the distribution and organization of CTL-oleate (Fig. 5C) in LDL, and by that approach, a temperature-dependent phase transition of the particle could be demonstrated.[109,111]

Another approach to the development of intrinsically fluorescent CEs is to use esters in which the fatty acid is fluorescent. Perhaps the best known examples are the esters of parinaric acid (trivial name for octadeca-9,11,13,15-tetraenoic acid—see Fig. 5D). The acid naturally occurs in a large quantity (46%) in Makita (*Parinari laurina*) seeds, from which it can be extracted and purified by repeated crystallization from petroleum ether.[112] Nowadays, it can also be obtained synthetically, either using α-linoleic acid as a starting molecule or by iterative cross-coupling.[113] Parinaric acid has been used as a fluorescent probe for membrane structure,[114,115] and also for many other kinds of studies, for example, to investigate human plasma lipoproteins.[116] Also its esters with cholesterol have been synthesized[105] and used, for example, as a probe for LDL structure.[109] However, we are not aware of any live-cell imaging study using cholesteryl parinaric acid. In contrast, DHE-oleate has been synthesized as outlined

above for CTL-oleate, inserted into atherogenic acetylated LDL, and monitored by UV-sensitive wide field imaging in murine macrophages.[48] Currently, we follow-up on that approach in our laboratory, where we routinely make CTL-oleate and -linoleate, reconstitute it into LDL particles, and follow their uptake and transport itineraries in living cells. For example, we are studying the transport of CTL-linoleate as part of LDL in human fibroblasts lacking functional NPC2 protein (Fig. 6). By applying iterative maximum-likelihood deconvolution, to reassign out-of-focus light to the correct planes in a 3D image stack, we achieve confocal-like sectioning capability of the microscope (data not shown).[29] Similarly, Richardson–Lucy (RL) maximum-likelihood deconvolution can be applied to single CTL images and gives improved resolution, in which individual peripheral vesicles containing CTL can be clearly discerned (Fig. 6B, upper and middle panel).[117] We chose this algorithm, as implemented in the Deconvolution lab plugin to ImageJ, since it provides an accurate description of image noise as a Poisson statistics and gave the best results in our hands.[117–119] The extent of blurring of an object by the microscope objective lens can be understood by considering the lens as a low-pass filter meaning that only spatial frequencies of the diffracted light up to a certain cutoff can pass the lens.[117] Deconvolution is sometimes called computational super-resolution, since it theoretically allows for reconstruction of spatial frequencies lying outside the support of the optics.[118,120] Even if this is rarely achieved in practice, deconvolution almost always improves image fidelity to some extent, since the practically achieved resolution is affected by other factors including the spatial sampling, eventual aberrations, as well as contrast and noise levels.[117,121] The performance of a deconvolution algorithm can be assessed not only from the visual image *improvement* but can also be judged by comparing the frequency representation of raw and deconvolved images, ie, their (fast) Fourier transform (FFT; Fig. 6B, lower panel).[117,118] Instead of spatial pixel coordinates (x, y), one gets frequency pixel coordinates (u, v). Zero frequencies are found in the center of those 2D spectra and increasing frequencies toward the edges (Fig. 6B, lower panel). The *intensities* in the FFT spectra tells how much each frequency is represented in the respective image (ie, the amplitude). With this in mind, inspection of the FFT spectra clearly shows that RL deconvolution gives a larger contribution of higher spatial frequencies (ie, higher values in the periphery of the FFT maps). Such higher frequencies correspond to finer spatial details in the fluorescence images. Thus, with 20–40 iterations of the RL algorithm, we indeed improve the resolution compared with the raw images, thereby partly compensating for out-of-focus blurring and other factors (Fig. 6B). The deconvolution outcome is so convincing here, because the cells take up significant amounts of labeled LDL, resulting in a high CTL signal and thereby a good signal-to-noise ratio. Thus, we see in independently acquired bleach stacks as well as in direct comparison with unlabeled fibroblasts that the CTL signal is 7–10-fold that of the autofluorescence (data not shown).[62,122] In this way, we demonstrated that after hydrolysis of the ester, some of the liberated CTL is able to reach the PM with many small cytoplasmic vesicles in the cell periphery. The majority of CTL gets trapped in perinuclear LE/LYSs due to a lack of functional NPC2 protein in these cells (Fig. 6 and Solanko et al, manuscript in preparation). These initial results clearly support the huge potential of wide field deconvolution imaging of P-sterol esters for analysis of lipoprotein-mediated cholesterol transport pathways in health and disease.

Extrinsic Cholesterol Analogs

Recently, several different extrinsic cholesterol analogs have been synthesized. However, some of them appear to be very artificial with respect to their ability of mimicking cholesterol, or they have not been used for trafficking studies so far. Accordingly, they are not going to be discussed in this review. In the following section, we focus on the closest analogs of cholesterol, bearing a tagged fluorescent group.

BODIPY-tagged cholesterol and CE analogs. Boradiaza-indacene (BODIPY)-tagging is a versatile and common approach for generating fluorescent lipid probes with preferable photophysical properties together with acceptable impact on the native lipid structure.[123] BODIPY-cholesterol was first introduced by Li et al in 2006,[124] and this cholesterol analog became well accepted by the research community shortly after (eg, in Ref. 49 and recently reviewed in Ref. 125). Li et al have synthesized several BODIPY-tagged cholesterol derivatives. The first were obtained by coupling a carboxyl acid derivative of BODIPY with a sterol analog containing a hydroxyl group at the side chain, mediated by the coupling reagent *N*,*N*′-dicyclohexylcarbodiimide (DCC)—thus giving an ester link.[124] A different approach involves Suzuki or Liebeskind–Srogl coupling—in that case, instead of an ester group an aryl ring acts as a linker.[126] Only two of them (Fig. 7A and D) partition preferentially into the cholesterol-rich lo phase in ternary model membranes.[87,88,127,128] In GUVs made of dipalmitoyl phosphatidylcholine (DPPC), dioleoyl phosphatidylcholine, cholesterol (Fig. 1A), DHE (Fig. 3B), BODIPY-cholesterol (Fig. 7A), and the ld marker di-C12-indocarbocyanine (DiIC12), the different extent of lo preference of both fluorescent sterol probes could be directly visualized by multicolor wide field imaging in the same membrane.[88] So far, no other extrinsically tagged fluorescent cholesterol analogs than the two BODIPY-cholesterol derivatives shown in Figure 7A and D were reported to show preferred partitioning into the lo phase.[127] This key property together with the overall comparable trafficking kinetics and itineraries from the PM as DHE and at least 600-fold higher brightness compared with CTL or DHE make BODIPY-tagged cholesterol analogs the preferred extrinsic cholesterol analog.[125] In particular, their high photostability under two-photon excitation makes the BODIPY-cholesterol probes shown in Figure 7A and D very attractive for long-term time-lapse imaging and fluorescence

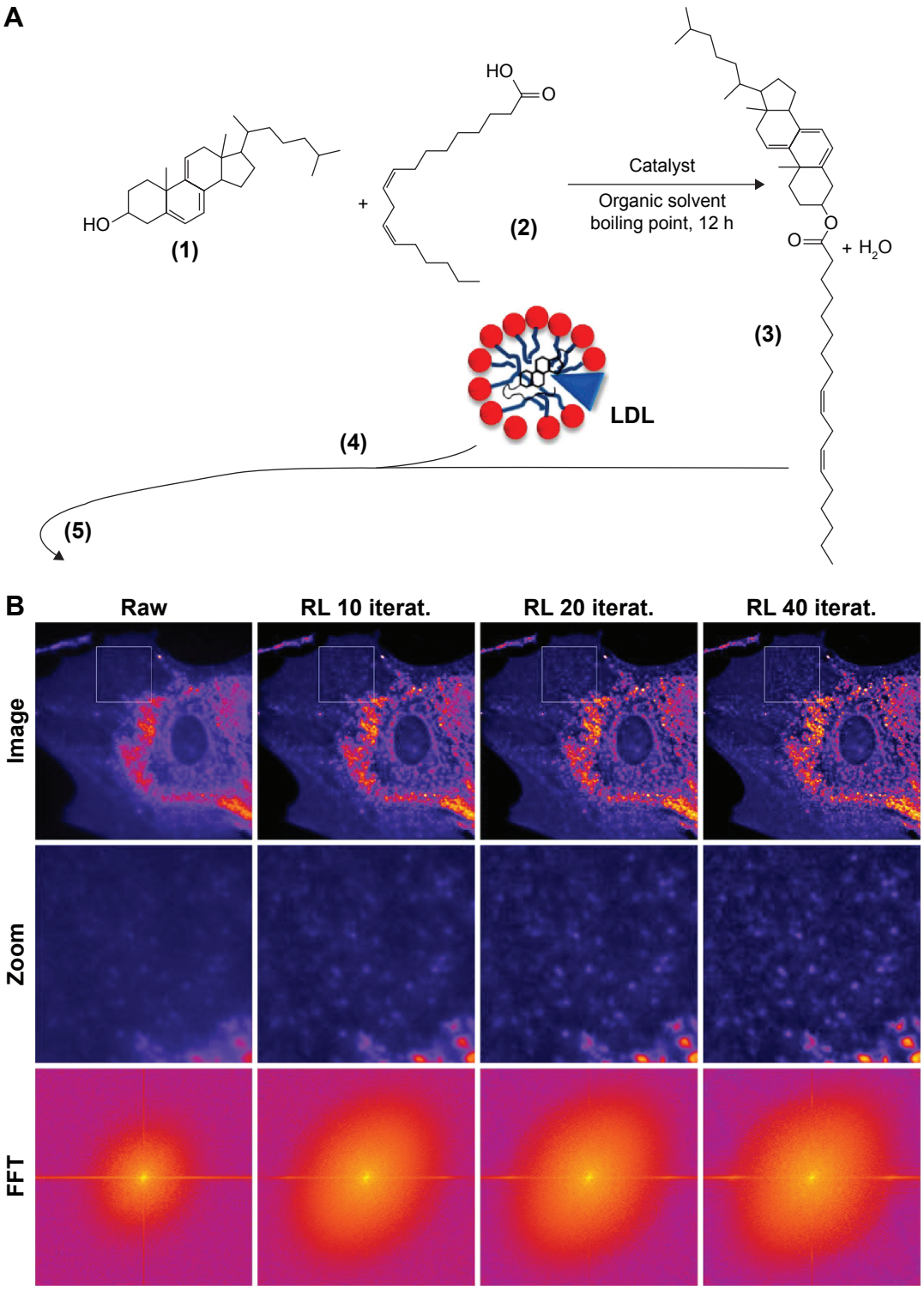

Figure 6. Direct observation of CTL ester processing after ingestion of LDL in Niemann–Pick C2 fibroblasts. (**A**) The esterification reaction of CTL (**1**) with linoleate (**2**) to CTL-linoleate (**3**) and water followed by reconstitution of CTL-linoleate into LDL (**4**) for imaging in cells (**5**). NPC2 disease fibroblasts were incubated in the medium containing CTL-linoleate reconstituted into LDL as the only lipoprotein source for 24 hours. Cells were washed and imaged on a UV-sensitive wide field microscope equipped with z-stacking capability for acquiring multiple images along the optical axis. (**B**, upper row, "Image"): CTL image as acquired ("Raw") or after various iterations of RL deconvolution. Especially after deconvolution, CTL fluorescence in LE/LYSs, the perinuclear region, and the PM can be discerned. In addition, the inset being enlarged in the middle panel (**B**, "Zoom") reveals many small peripheral vesicles containing CTL, again clearly visible after RL deconvolution for 20–40 iterations. The improved image quality can also be judged from the frequency representation of the images, ie, their Fourier transform (**B**, lower panel, "FFT"). Herein, the contribution of higher spatial frequencies (ie, higher values in the periphery of the FFT maps) is apparent after deconvolution. Higher frequencies in the FFT maps correspond to finer details in the images, indicating that maximum-likelihood deconvolution efficiently removes out-of-focus blur, resulting in higher contrast and resolution. This is essential for detecting sterol in small vesicles and other structures. Images are shown color-coded with a FIRE-LUT.

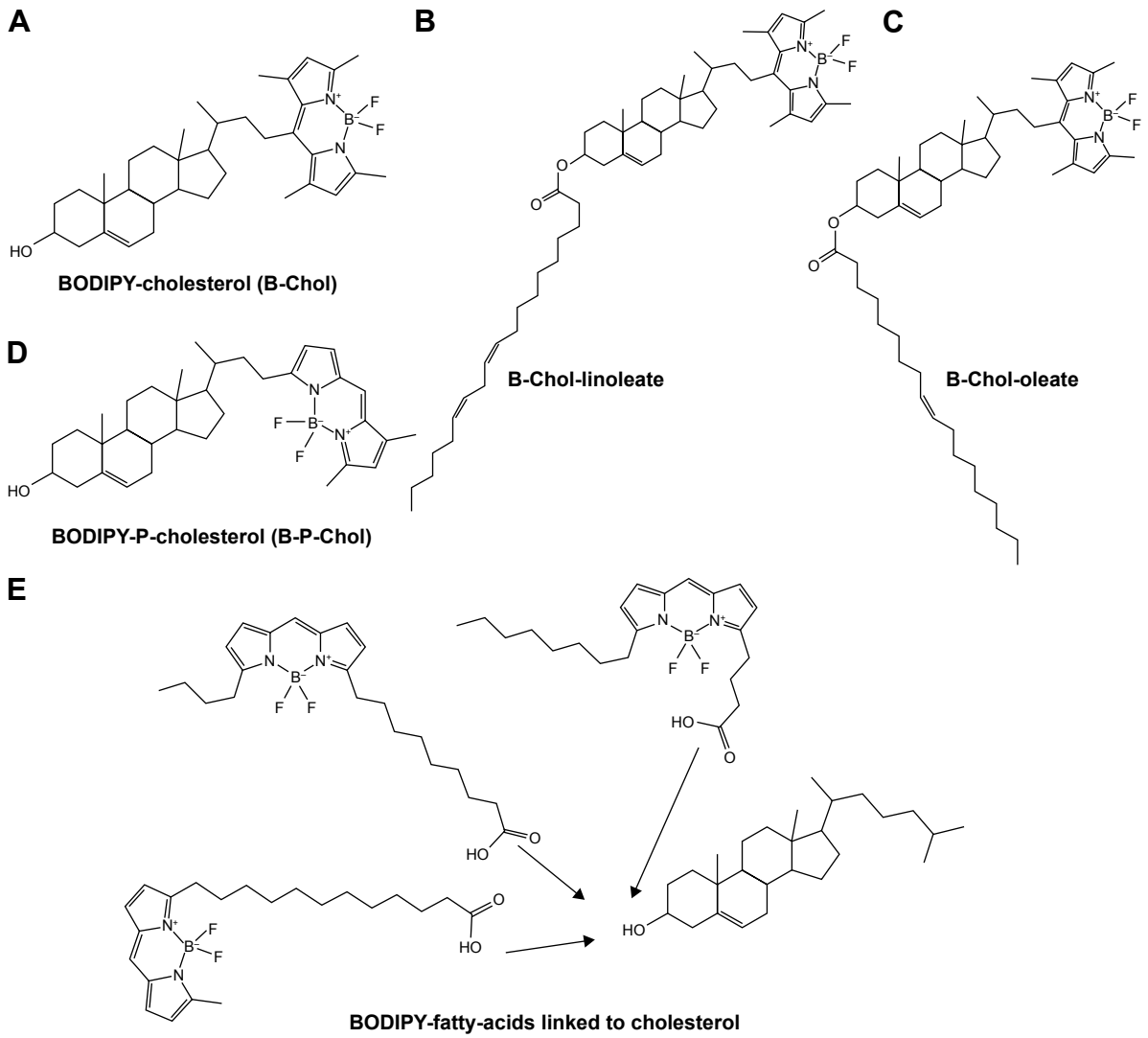

Figure 7. Structure of BODIPY-tagged cholesterol analogs, their esters, and BODIPY-fatty acids, which can be esterified to cholesterol. Commercially available BODIPY-cholesterol (**A**, TopFluor-cholesterol from Avanti), its ester with linoleate (**B**), or with oleate (**C**). Hydrolysis of such esters in cells allows one to follow the fate of the tagged cholesterol moiety. BODIPY-P-cholesterol (**D**) is a probe in which the BODIPY group is linked to cholesterol's side chain via one of the pyrrole rings of the dye. Three different BODIPY-labeled fatty acids have been linked to cholesterol to produce a fluorescent ester (**E**). Hydrolysis of such esters in cells enables one to follow the fate of the tagged fatty acid moiety.

correlation spectroscopy in living cells.[129] They are also useful for assessment of probe orientation by two photon-based fluorescence polarimetry in models and cell membranes.[128] In addition, BChol and B-P-Chol have been used to determine diffusion laws of lo preferring cholesterol analogs in the PM of living cells, either using high-speed single-molecule tracking or based on stimulated emission depletion microscopy coupled to fluorescence correlation spectroscopy.[128,130] Fast and mostly free, unhindered diffusion of both cholesterol analogs down to a spatial scale of <80 nm in both leaflets of the PM was found by such advanced imaging approaches. Thus, the prediction of the raft hypothesis, namely, trapping of cholesterol analogs in the PM, could not be confirmed. Similar results were found with a PEG-linked extrinsic cholesterol analog in various cells including cells grown on patterned surfaces.[131,132] Further discussion of that topic can be found in a recent review.[100] Interestingly, we found that the orientation of the BODIPY-moiety has no impact on phase preference or lateral diffusion of BOIPY-tagged cholesterol probes in model membranes, but affects their lateral diffusion in the PM of living cells, where B-P-Chol diffuses almost twice as fast as BCol.[128] Also, BODIPY-tagged cholesterol probes, as those shown in Figure 7A and D, accumulate to an artificial extent in LDs of fatty acid loaded cells.[88,133] This is a direct consequence of the dye chemistry, since BODIPY is a prominent LD marker.[134] Including a linker between cholesterol's alkyl chain and the BODIPY group caused preferred partitioning of such analogs into the ld phase in model membranes and rapid nonspecific redistribution to several organelle membranes in living cells.[88,127,135] Thus, the attachment and orientation of the fluorophore in extrinsic cholesterol analogs can have dramatic effects on their distribution and diffusion in living cells.

Milles et al studied cholesterol dynamics in models and cell membranes using several BODIPY-tagged cholesterol analogs including the one shown in Figure 7A.[135] They have also investigated the interaction between cyclodextrin and cholesterol analogs and related that property to the ordering capacity of the probes in POPC membranes, as assessed by NMR spectroscopy. Importantly, despite having the lowest extractability from membranes to cyclodextrin of all studied extrinsic cholesterol analogs, BODIPY-cholesterol (Fig. 7A) had no ability to order fatty acyl chains in POPC bilayers.[135] This is an important and somehow alarming observation, since it shows that a crucial property of cholesterol—to condense lipid bilayers—vanishes when an extrinsic dye is linked to the sterol molecule. In similar studies carried out by the same research team, only CTL and—to a lower extent—DHE were able to order fatty acyl chains in POPC membranes, reiterating the close resemblance of cholesterol by these P-sterols.[53] The BODIPY-tagged cholesterol shown in Figure 7A is commercially available from Avanti Polar Lipids under the name TopFluor-cholesterol, and it has also been used for in vivo imaging after injecting the probe into the zebrafish egg yolk sack for subsequent observation over several days.[49] Such studies could be well supplemented by two-photon excitation microscopy with all its advantages of probe imaging in thick samples.

BODIPY-cholesteryl-oleate and -linolate with the fatty acids coupled to the 3′-hydroxy group of BODIPY-tagged cholesterol have been recently introduced by Kanerva et al for tracking the LDL pathway of cholesterol import into cells (Fig. 7B and C).[136] Both linoleic and oleic acids are naturally occurring in cells and in the esterified form of cholesterol. There is a widely known protocol how to reconstitute LDL with either fluorescent or radioactive CEs, which was also used for incorporating BODIPY-cholesteryl-oleate and -linolate into LDL.[136,137] Even though the BODIPY-cholesteryl-esters were transported to LE/LYSs, hydrolysis of these probes was found to be much slower than that of native CEs.[136] Thus, it is likely that the BODIPY group interferes sterically with acid lipase activity, thereby causing diminished hydrolysis of the BODIPY-tagged CEs. BODIPY-cholesteryl-oleate has also been used by Röhrl et al to follow selective uptake pathways of CEs from HDL in the hepatocyte-like cell line HepG2.[138] Similar to CEs with a fatty acyl-linked BODIPY group, the fluorescent ester remained associated with HDL for prolonged time after holo-particle endocytosis.[138,139] It remains to be determined whether this trafficking route indeed resembles that of native CEs or is biased by the bulky BODIPY group. For that purpose, P-sterol esters, such as CTL-linoleate, could be incorporated into HDL and studied in polarized HepG2 cells or other hepatocyte model systems.[140] Further details about BODIPY-tagged CEs can be found in recent reviews.[125,141]

6-Dansyl-cholesterol. Dansyl (5-dimethylamino-1-naphthalenesulfonyl) as a fluorophore is commonly applied to tag lipids, proteins, and other biomolecules, due to its environmental sensitivity, solvent polarity, and a long lifetime.[142] A cholesterol analog bearing the dansyl group attached at the sixth carbon of cholesterol was originally synthesized by Wiegand et al, by condensing 6-ketocholestanol with dansyl hydrazine catalyzed by HCl.[143] Due to the specific linkage at carbon 6, the double bond of cholesterol is removed, and the resulting probe is a Dansyl-cholestanol (DChol; Fig. 8A). DChol was first used to study sterol trafficking in CT43 cells, CHO mutants deficient in a functional NPC1 protein. There, it was found that DChol is esterified similar to cholesterol.[143] DChol has a broad excitation and emission spectrum with maxima around 336 and 522 nm, respectively. The fluorophore is small and exhibits relatively high quantum yield, but it is prone to photobleaching similar to that of P-sterols, filipin, or NBD-tagged cholesterol analogs. The emission of DChol is environmentally sensitive and shift toward lower wavelengths (around 509 nm) at neutral pH in polar solvents. When dropped to pH of approximately 1–2, the emission intensity at 509 nm decreases with an additional shift of DChol's maximum peak toward 490 nm. Fluorescence of Dansyl-tagged lipids is highly influenced by the polarity of the solvent, and its emission maximum can be red-shifted by 26 nm when the solvent dielectric constant (D_{solv}) increases from 2 to 42. Also, in the range of D_{solv} = 2–40, the Stokes shift of DChol is proportional to D_{solv}, in line with the Onsager theory and the Lippert–Mataga equation.[142,143] Further increasing solvent polarity to D_{solv} = 80 gave only a minor blue shift of 4 nm, indicating the formation of micelles or microcrystals of DChol in such solvents.[144] This was confirmed by light scattering and fluorescence polarization measurements in the same study, giving a critical micelle concentration of 155 nM for DChol compared to ≤35 nM for cholesterol.[144,145] Monitoring the shifts in excitation and emission maxima combined with fluorescence lifetime and anisotropy measurements as readout for membrane packing has also been used for other Dansyl-tagged lipids, such as Dansyl-tagged phosphatidyl ethanolamine (DPE) and phosphatidylserine (DPS).[142,146] The mean fluorescence lifetime of DChol was calculated by fitting a triexponential decay function to the intensity decay of DChol in POPC liposomes to be 13.2 nsec.[147] In membranes made of DPPC, DChol's mean lifetime increased to ~15.6 nsec, while it was intermediate (14.6 nsec) in liposomes mimicking the lo phase (ie, DPPC with 40 mol% of cholesterol).[147] Also the fluorescence anisotropy and apparent rotational correlation time of DChol were sensitive to the lipid phase in these liposomes.[147] In the same study, analysis of the membrane penetration depth of the Dansyl group based on parallax quenching by nitroxy-tagged lipid probes revealed that the average localization of the fluorophore attached to the sterol ring system is ~15.6 Å from the center of the bilayer.[148] These findings are in line with the previous studies using neutron diffraction to localize cholesterol in the phospholipid membrane.[149] However, no partition preference of DChol between

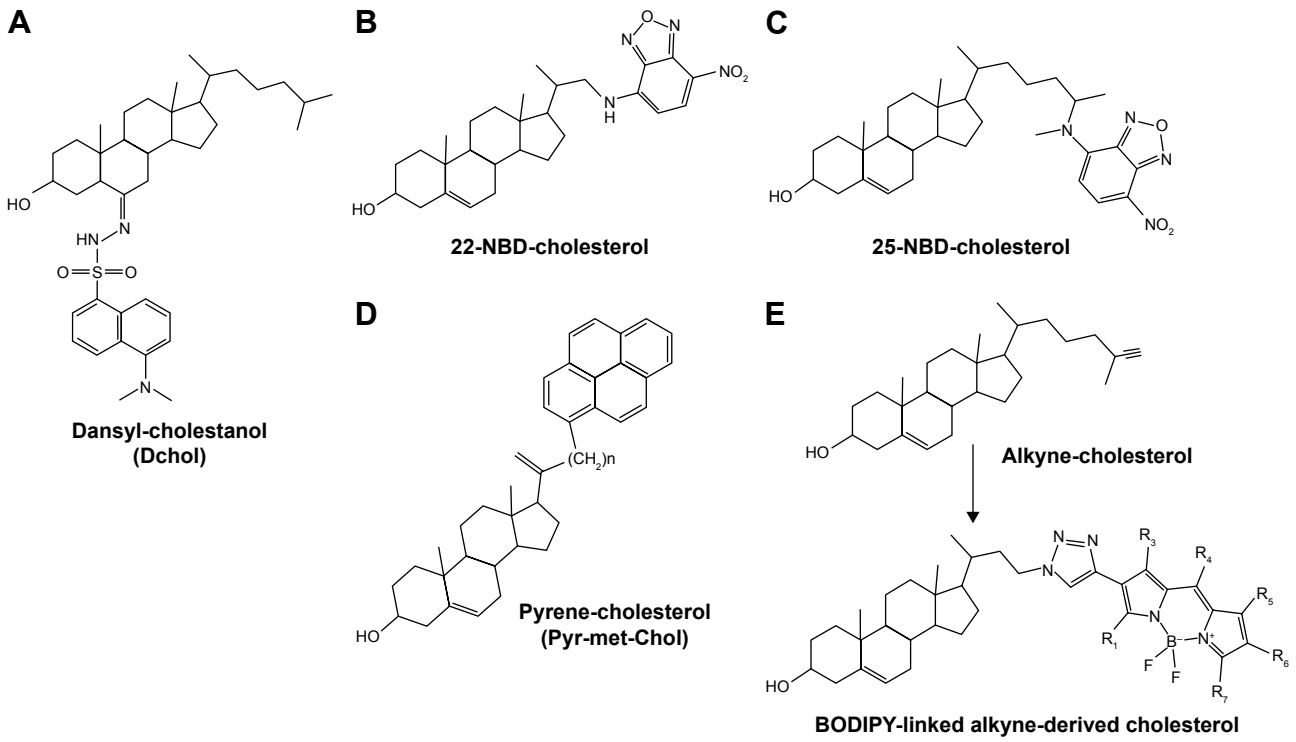

Figure 8. Structure of additional extrinsically fluorescent cholesterol analogs. 6-Dansyl-cholesterol (**A**, DChol), 22-NBD-cholesterol (**B**), 25-NBD-cholesterol (**C**), pyrene-tagged cholesterol analogs (**D**, when $n = 2$, it is called Pyr-met-Chol as described in the text). (**E**) Alkyne cholesterol can be chemically linked to various fluorescent dyes including BODIPY when provided as azido derivative. See text for further explanations.

ordered and disordered membrane phases has been shown in these studies. DChol has been inserted into the membranes of living cells by one of the three methods: (a) directly from the culture media in which the sterol was dissolved with an incubation of approximately 1–2 hours, (b) as a complex with β-cyclodextrin with a short incubation of 2–30 minutes,[143,144] and (c) as part of large unilamellar vesicles composed of POPC: DChol.[150] Since the excitation spectrum of the Dansyl group shows a strong spectral overlap with the emission of DHE, Förster resonance energy transfer (FRET) occurs between both types of fluorophores. This has been used initially in spectroscopic experiments to study lipase activity and cholesterol solubilization by bile salts and determine flip-flop rates for DHE in liposomes, always with Dansyl-tagged lipids such as PC or DPE as FRET acceptors.[151–153] Huang et al used FRET between DHE and DChol, which was detected by sensitized emission after multiphoton excitation of the DHE donor in intact cells.[144] Close proximity of both fluorescent sterols was inferred from FRET taking place in selected regions of the PM. Despite these and similar promising studies, it must be emphasized that the Dansyl group protrudes from the sterol backbone and will likely disturb cholesterol-induced membrane condensation significantly. In fact, DChol partitions with high preference into the cholesterol-poor ld phase in model membranes and colocalized little with cholesterol-rich LE/LYSs in NPC1 disease cells.[97] These results, together with the high bleaching propensity of this probe, make the use of DChol for live-cell imaging studies on cholesterol transport questionable.

NBD-tagged cholesterol analogs. Cholesterol analogs bearing a 7-nitrobenz-2-oxa-1,3-diazole (NBD) group at either carbon 22 (Fig. 8B) or 25 of cholesterol (Fig. 8C) share some properties with DChol. They have similar environmental sensitivity of emission, suitable brightness, and also high bleaching propensity, and such probes have been widely used in cellular studies for more than 30 years.[154,155] 22- and 25-NBD-cholesterol can be easily incorporated into cells by direct addition from media, with the help of β-cyclodextrin or serum albumin present in the medium, both for cholesterol-trafficking studies in mammalian cells and fungi.[156–158] This is partly a consequence of their higher water solubility and much faster intermembrane exchange compared with cholesterol, ergosterol, or P-sterols.[159] In fact, both NBD-tagged cholesterol analogs showed a mean half-time for a passive exchange of 10–120 seconds, similar to side-chain oxysterols, but in stark contrast to cholesterol, DHE, or CTL, with exchange half-times in the range of 45 minutes to 1 hour in fluid PC membranes.[102,159–161] Both 22- and 25-NBD-cholesterol have a strong tendency to orient opposite to cholesterol in lipid bilayers; they have no capacity to order fatty acyl chains of POPC, and they partition exclusively into the ld phase in ternary model membranes, in stark contrast to cholesterol.[53,89,127,135] Despite these strong deviations from cholesterol's behavior, 25- (but not 22-) NBD-cholesterol could be used to monitor the

physical properties of cell membranes depleted of cholesterol.[162] Such experiments have been carried out in a straightforward way by lifetime imaging, as the increased hydration of 25-NBD-cholesterol upon cellular cholesterol depletion gave a change in mean fluorescence lifetime of ~0.7 nsec.[162] Prolonged time-lapse imaging, FRAP, or FLIP studies are more difficult to carry out with 22- and 25-NBD-cholesterol, as both analogs are significantly less bright and photostable than BChol.[97] When 25-NBD-cholesterol was introduced into CHO cells from culture media, it did not show prominent PM staining and became miss-targeted to cholesterol-poor mitochondria.[163] Interestingly, also in yeast, mitochondria have been implicated in the uptake of 25-NBD-cholesterol, and both 22- and 25-NBD-cholesterol were shown to serve as substrates for mitochondrial monooxygenases in yeast.[164,165] Thus, the preferred uptake and transport of both cholesterol analogs to mitochondria in mammalian and fungal cells could be a consequence of metabolic trapping and conversion of the NBD group into 7-nitrobenz(1,2,5)oxadiazole-4-amine.[164] Also, the NBD group affects the cellular efflux of the tagged cholesterol probe, as 22-NBD-cholesterol is released from cells to HDL in the medium with rates much higher than those for ^{3}H-cholesterol.[166] While 22-NBD-cholesterol is esterified by ACAT to a higher extent than cholesterol,[61,145] the extent of esterification of this probe is linearly proportional to that of native cholesterol.[167,168] When incorporated into LDL, 22-NBD-cholesterol was also found to be able to efficiently downregulate the expression of HMGR.[155] Thus, for some metabolic investigations, such as studying ACAT activity in cells, 22- and 25-NBD-cholesterol seem to be useful. In contrast, the majority of biophysical studies applying these NBD-tagged cholesterol analogs picture these probes as poor mimics of cholesterol in biological membranes. Even though 25-NBD-cholesterol seems to be useful for studying sterol uptake in yeast,[158,169] P-sterols such as DHE differing from the yeast sterol ergosterol only in one additional double bond will outperform extrinsically tagged sterol also in such uptake assays.[46,47]

Pyrene-tagged cholesterol and its esters. When pyrene-containing lipids assemble in close proximity, the pyrene groups show a characteristic red-shifted excited state emission (excimer). This property has been used in many different applications, for example, in the case of acyl chain labeled pyrene CEs, to study their exchange between HDL particles catalyzed by a transfer protein.[170] The same probe inserted into LDL was used to follow trafficking and lysosomal degradation of CEs in human fibroblasts.[171] When reconstituting LDL with both cholesteryl-linoleate and cholesteryl-decanyl-pyrene, both were similarly hydrolyzed by acid lipase in a concentration-dependent manner, and the pyrene-tagged decanate was able to leave the LE/LYSs in control but not in Wolman disease fibroblast, which lack the lipase.[171] These studies suggest that CEs tagged in the acyl chain with a pyrene group are suitable surrogates of native CEs, also for UV-sensitive imaging application. A few years later, in 2007, a cholesterol derivative with the pyrene attached to the alkyl chain has been introduced and named 21-methylpyrenyl-cholesterol (Pyr-met-Chol; Fig. 8D).[172] This compound was obtained by a condensation reaction between 1-pyrenecarboxaldehyde and pregnenolone. Pyr-met-Chol was shown to be easily incorporated into membranes where it has a tendency to self-associate, which again was assessed by measuring the extent of excimer formation.[172] It cannot be ruled out that self-association of Pyr-met-Chol is a direct consequence of stacking of the bulky fluorophore within the bilayer. Partitioning experiments of Pyr-met-Chol between the lo and ld phase in ternary lipid membranes have not been reported, but it is possible that the pyrene group significantly perturbs the bilayer and thereby conflicts with the cholesterol-induced membrane condensation, as shown for other pyrene-tagged lipids.[173] Pyr-met-Chol can be introduced into lipoproteins, which function as a vehicle for delivering this probe to cells.[174] After labeling, Pyr-met-Chol showed strong intracellular accumulation, which is in contrast to cholesterol which is known to reside mostly in the PM.[175] Also in contrast to cholesterol and also to analogs such as DHE, CTL or BODIPY-cholesterol is the complete absence of esterification of Pyr-met-Chol in cells. Together, the potential of pyrene-tagged sterol probes to report about eventual local sterol enrichment by excimer formation is counterbalanced if not overshadowed by the limited resemblance of cholesterol's properties in cells.

Click chemistry strategy and derivatives of alkyne cholesterol. A strategy aimed at using the benefits of both extrinsically and intrinsically fluorescent sterol analog bases on the so-called *click chemistry* reactions. Click chemistry is a concept of using high-yield reactions for joining functional chemical groups in a reliable and quick way. Perhaps the best known click chemistry reaction is the azide alkyne Huisgen cycloaddition, in which an azide group reacts with an alkyne group in the presence of Cu^{+} ions (usually generated in situ) to form a substituted 1,2,3-triazole ring.[176] This approach was used for analyzing lipids. It turned out that fatty acids bearing an alkyne group are treated by living cells just like natural fatty acids, but they are much easier to detect and visualize on TLC plates, for example, after in vitro enzymatic assays.[177,178] A similar principle was also applied to the analysis of sterols. Again, it was proven that alkynated analogs of sterols are treated by the organism like native sterols—with respect to both distribution and susceptibility to enzymatic reactions.[179,180] Moreover, click chemistry provides a broad range of possibilities for detecting and analyzing the sterols, ranging from TLC over UV/Vis detection and fluorescence microscopy to mass spectrometry and Raman microscopy (including coherent anti-Stokes Raman scattering [CARS] microscopy).[133,179,181] In the latter case, C≡C stretching vibrations were amplified by generating a conjugated system of π-electrons from the alkyne group to a linked phenyl ring in the side chain of cholesterol. This allowed for

detection of the resulting cholesterol probe in living cells and in *Caenorhabditis elegans*.[133] The phenyl-tagged Raman-active cholesterol probe accumulated in LE/LYSs of Niemann–Pick C1 mutant cells and was not cytotoxic due to a protecting effect of the terminal phenyl group.[133] Cytotoxicity became an issue for the used alkyne cholesterol in the same study, which differs slightly from the one used by the Thiele group.[133,179] In fact, the latter probe contained the alkyne at the end of cholesterol's side chain (Fig. 8E) and showed no cytotoxicity, neither in mammalian cells nor in yeast cells.[179] The slightly shortened aliphatic chain used in the alkyne cholesterol by Lee et al[133] might be treated differently in cells, which is in line with the biophysical studies on the importance of cholesterol's side chain for its membrane properties.[182,183] An additional advantage of Raman-active cholesterol probes, such as the phenyl-tagged alkyne cholesterol, is the fact that they can be visualized by CARS or stimulated Raman microscopy. These methods can be easily combined with other nonlinear optical imaging techniques, such as multiphoton excitation fluorescence microscopy.[133,184] When given to CHO cells, phenyl-tagged alkyne cholesterol became enriched in LDs only upon esterification by ACAT, very much like DHE and CTL but in stark contrast to BODIPY-cholesterol, which accumulates in LDs without esterification due to the preferred partitioning of the BODIPY group into that organelle.[51,73,88,133] Note that for these Raman studies, cells or nematodes were incubated with the phenyl-tagged alkyne cholesterol, so that no additional click chemistry reaction was necessary. This is in contrast to the fluorescence imaging studies using alkyne cholesterol mentioned above. Very recently, a new alkyne cholesterol and alkyne 25-hydroxycholesterol probe has been presented, in which the alkyne replaces the axial methyl group at carbon 19 of the sterols (structure not shown, but compare Figs. 1A and 8E).[185] The 19-ethynyl-cholesterol (eChol) supported Hedgehog signaling similar to cholesterol and was detected by fluorescein-azide after click reaction in the PM and to a lower extent in the ER and mitochondria.[185] Also, eChol could rescue the growth defect of the partially sterol auxotroph CHO cell line M19 similar to cholesterol.[185] Since the same group also studies other alkyne-tagged lipids, two-color imaging of eChol with alkyne choline phospholipids could be performed in the same study. However, it has to be noted that even though the presented alkyne cholesterol analogs differ very little from cholesterol, the finally visualized sterol distribution is based on an extrinsic analog, in which a bulky fluorophore becomes linked to the alkyne group. Accordingly, all concerns about reliability of extrinsic fluorescence probes for cholesterol, as discussed in detail above, applies also to alkyne-tagged cholesterol analogs. Also, for using the classic Huisgen cycloaddition in such applications, cells need to be fixed before the addition of the tag, as copper (I) is cytotoxic, so, it is not possible to conduct fluorescence microscopy analysis of alkyne-tagged cholesterol analogs in living cells. However, there are other types of so-called *biorthogonal* click reactions that can be used to conjugate the alkyne with a fluorophore in living cells, for example, conjugation with strained cyclooctynes[186]—this approach has been used for in vivo imaging of glycan[187] and is currently under investigation for possible application to sterols.[180]

Summary and Outlook

We have described three main approaches to cholesterol imaging in cells by fluorescence microscopy: applying intrinsically or extrinsically fluorescent cholesterol analogs and using alkyne cholesterol derivatives acting as a substrate for click chemistry reactions introducing the fluorophore. All three approaches have benefits and drawbacks. For example, while intrinsically fluorescent sterols usually mimic natural cholesterol much better than extrinsically fluorescent ones; they also have a much lower molecular brightness and emit UV light and, therefore, require more specific equipment and very sensitive cameras for detection. On the other hand, applying the alkyne derivatives bears the potential of combining the best properties of intrinsically and extrinsically fluorescent derivatives. However, in this approach, the cells need to be fixed, and the most widely used click chemistry catalyst, Cu (I) ions, is cytotoxic. Also, the finally detected sterol probe is again an extrinsic cholesterol analog in this technique, and it has not yet been shown that the fluorophore has equal access to the ethynyl group in all cellular membranes during the click reaction step.

We are left with a *toolbox* of various molecules that are suited to different applications, ranging from in vivo sterol tracking to enzymatic assays. However, the situation changes dynamically, and it is possible that, with advances in synthetic chemistry, new cholesterol probes become available. For example, the development of biorthogonal click reactions could allow researchers soon to link dyes to alkyne cholesterol under more physiological conditions. Similarly, intrinsically fluorescent alkyne cholesterol analogs could be synthesized, for example, CTL with the ethynyl group at position C26, thereby enabling one to assess whether the click reaction takes place equally well in all cellular membranes. Finally, the fluorescence properties of intrinsically fluorescent analogs can be improved by introducing a fourth conjugated double bond in the steroid ring system. This has been predicted to red-shift the excitation and emission maxima and increase the extinction coefficient sufficiently to image such probes with conventional microscope instrumentation.[80] This would eventually allow for detecting sterol transport to organelles with lower cholesterol abundance, such as ER, Golgi, or mitochondria. Together, we have recently witnessed rapid progress in synthetic and computational chemistry of suitable cholesterol analogs. These developments combined with the fast improvement of live-cell imaging technology and an increasing understanding of cholesterol's specific properties in membranes promise a bright future for in-depth analysis of cholesterol trafficking and its alterations in human disease.

Author Contributions

Conceived and designed the experiments: DW, KAS, LMS. Analyzed the data: DW. Wrote the first draft of the manuscript: DW, KAS. Contributed to the writing of the manuscript: KAS, MM, DW. Agree with manuscript results and conclusions: KAS, MM, LMS, DW. Jointly developed the structure and arguments for the paper: KAS, MM, DW. Made critical revisions and approved final version: MM, DW. All authors reviewed and approved of the final manuscript.

REFERENCES

1. Behrman EJ, Gopalan V. Cholesterol and plants. *J Chem Educ*. 2005;82:1791–1793.
2. Schroeder F, Barenholz Y, Gratton E, Thompson TE. A fluorescence study of dehydroergosterol in phosphatidylcholine bilayer vesicles. *Biochemistry*. 1987;26:2441–2448.
3. Marrink SJ, de Vries AH, Harroun TA, Katsaras J, Wassall SR. Cholesterol shows preference for the interior of polyunsaturated lipid membranes. *J Am Chem Soc*. 2008;130:10–11.
4. Aittoniemi J, Róg T, Niemelä P, Pasenkiewicz-Gierula M, Karttunen M, Vattulainen I. Tilt: major factor in sterols' ordering capability in membranes. *J Phys Chem B*. 2006;110:25562–25564.
5. Mesmin B, Maxfield FR. Intracellular sterol dynamics. *Biochim Biophys Acta*. 2009;1791:636–645.
6. Wüstner D, Solanko KA. How cholesterol interacts with proteins and lipids during its intracellular transport. *Biochim Biophys Acta*. 2015;1848:2188–2199.
7. Goldstein JL, DeBose-Boyd RA, Brown MS. Protein sensors for membrane sterols. *Cell*. 2006;124:35–46.
8. Sharpe LJ, Cook ECL, Zelcer N, Brown AJ. The UPS and downs of cholesterol homeostasis. *Trends Biochem Sci*. 2014;39:527–535.
9. Lange Y, Ye J, Rigney M, Steck TL. Regulation of endoplasmic reticulum cholesterol by plasma membrane cholesterol. *J Lipid Res*. 1999;40:2264–2270.
10. van Meer G, Voelker DR, Feigenson GW. Membrane lipids: where they are and how they behave. *Nat Rev Mol Cell Biol*. 2008;9:112–124.
11. Tabas I. Free cholesterol-induced cytotoxicity—a possible contributing factor to macrophage foam cell necrosis in advanced atherosclerotic lesions. *Trends Cardiovasc Med*. 1997;7:256–263.
12. Radhakrishnan A, Goldstein JL, McDonald JG, Brown MS. Switch-like control of SREBP-2 transport triggered by small changes in ER cholesterol: a delicate balance. *Cell Metab*. 2008;8:512–521.
13. Sokolov A, Radhakrishnan A. Accessibility of cholesterol in endoplasmic reticulum membranes and activation of SREBP-2 switch abruptly at a common cholesterol threshold. *J Biol Chem*. 2010;285:29480–29490.
14. Xu XX, Tabas I. Lipoproteins activate acyl-coenzyme A:cholesterol acyltransferase in macrophages only after cellular cholesterol pools are expanded to a critical threshold level. *J Biol Chem*. 1991;266:17040–17048.
15. Chang CCY, Chen J, Thomas MA, et al. Regulation and immunolocalization of Acyl-Coenzyme a-cholesterol acyltransferase in mammalian-cells as studied with specific antibodies. *J Biol Chem*. 1995;270:29532–29540.
16. Goldstein JL, Brown MS. The LDL receptor. *Arterioscler Thromb Vasc Biol*. 2009;29:431–438.
17. Norata GD, Ballantyne CM, Catapano AL. New therapeutic principles in dyslipidaemia: focus on LDL and Lp(a) lowering drugs. *Eur Heart J*. 2013;34:1783–1789.
18. Maxfield FR, Tabas I. Role of cholesterol and lipid organization in disease. *Nature*. 2005;438:612–621.
19. Mukherjee S, Maxfield FR. Lipid and cholesterol trafficking in NPC. *Biochim Biophys Acta*. 2004;1685:28–37.
20. Wang ML, Motamed M, Infante RE, et al. Identification of surface residues on Niemann-Pick C2 essential for hydrophobic handoff of cholesterol to NPC1 in lysosomes. *Cell Metab*. 2010;12:166–173.
21. Lloyd-Evans E, Platt FM. Lipids on trial: the search for the offending metabolite in Niemann Pick type C disease. *Traffic*. 2010;11:419–428.
22. Kruth HS, Comly ME, Butler JD, et al. Type C Niemann-Pick disease. Abnormal metabolism of low density lipoprotein in homozygous and heterozygous fibroblasts. *J Biol Chem*. 1986;261:16769–16774.
23. Pentchev PG, Comly ME, Kruth HS, et al. A defect in cholesterol esterification in Niemann-Pick disease (type C) patients. *Proc Natl Acad Sci U S A*. 1985;82:8247–8251.
24. Storch J. Niemann-Pick C2 (NPC2) and intracellular cholesterol trafficking. *Biochim Biophys Acta*. 2009;1791:671–678.
25. Subramanian K, Balch WE. NPC1/NPC2 function as a tag team duo to mobilize cholesterol. *Proc Natl Acad Sci U S A*. 2008;105:15223–15224.
26. Gallala HD, Breiden B, Sandhoff K. Regulation of the NPC2 protein-mediated cholesterol trafficking by membrane lipids. *J Neurochem*. 2011;116:702–707.
27. McCauliff LA, Xu Z, Li R, et al. Multiple surface regions on the Niemann-Pick C2 protein facilitate intracellular cholesterol transport. *J Biol Chem*. 2015;290(45):27321–27331.
28. Maekawa M, Fairn GD. Complementary probes reveal that phosphatidylserine is required for the proper transbilayer distribution of cholesterol. *J Cell Sci*. 2015;128:1422–1433.
29. Maxfield F, Wüstner D. Analysis of cholesterol trafficking with fluorescent probes. *Methods Cell Biol*. 2012;108:367–393.
30. Nagao T, Qin C, Grosheva I, Maxfield FR, Pierini LM. Elevated cholesterol levels in the plasma membranes of macrophages inhibit migration by disrupting RhoA regulation. *Arterioscler Thromb Vasc Biol*. 2007;27:1596–1602.
31. Pipalia NH, Huang A, Ralph H, Rujoi M, Maxfield FR. Automated microscopy screening for compounds that partially revert cholesterol accumulation in Niemann-Pick C cells. *J Lipid Res*. 2006;47:284–301.
32. Bartz F, Kern L, Erz D, et al. Identification of cholesterol-regulating genes by targeted RNAi screening. *Cell Metab*. 2009;10:63–75.
33. Ishitsuka R, Saito T, Osada H, Ohno-Iwashita Y, Kobayashi T. Fluorescence image screening for chemical compounds modifying cholesterol metabolism and distribution. *J Lipid Res*. 2011;52:2084–2094.
34. Möbius W, Ohno-Iwashita Y, van Donselaar EG, et al. Immunoelectron microscopic localization of cholesterol using biotinylated and non-cytolytic perfringolysin O. *J Histochem Cytochem*. 2002;50:43–55.
35. Orci L, Montesano R, Meda P, et al. Heterogeneous distribution of filipin—cholesterol complexes across the cisternae of the Golgi apparatus. *Proc Natl Acad Sci U S A*. 1981;78:293–297.
36. Severs NJ, Simons HL. Failure of filipin to detect cholesterol-rich domains in smooth muscle plasma membrane. *Nature*. 1983;303:637–638.
37. Behnke O, Tranum-Jensen J, van Deurs B. Filipin as a cholesterol probe. I. Morphology of filipin-cholesterol interaction in lipid model systems. *Eur J Cell Biol*. 1984;35:189–199.
38. Behnke O, Tranum-Jensen J, van Deurs B. Filipin as a cholesterol probe. II. Filipin-cholesterol interaction in red blood cell membranes. *Eur J Cell Biol*. 1984;35:200–215.
39. Arthur JR, Heinecke KA, Seyfried TN. Filipin recognizes both GM1 and cholesterol in GM1 gangliosidosis mouse brain. *J Lipid Res*. 2011;52:1345–1351.
40. Smith RJ, Green C. The rate of cholesterol 'flip-flop' in lipid bilayers and its relation to membrane sterol pools. *FEBS Lett*. 1974;42:108–111.
41. Davenport L, Kutson JR, Brand L. Excited-state proton transfer of equilenin and dihydroequilenin: interaction with bilayer vesicles. *Biochemistry*. 1986;25:1186–1195.
42. Schroeder F. Fluorescent sterols—probe molecules of membrane-structure and function. *Prog Lipid Res*. 1984;23:97–113.
43. McIntosh AL, Atshaves BP, Huang H, Gallegos AM, Kier AB, Schroeder F. Fluorescence techniques using dehydroergosterol to study cholesterol trafficking. *Lipids*. 2008;43:1185–1208.
44. Ano Y, Kutsukake T, Hoshi A, Yoshida A, Nakayama H. Identification of a novel dehydroergosterol enhancing microglial anti-inflammatory activity in a dairy product fermented with *Penicillium candidum*. *PLoS One*. 2015;10:e0116598.
45. McIntosh AL, Gallegos AM, Atshaves BP, Storey SM, Kannoju D, Schroeder F. Fluorescence and multiphoton imaging resolve unique structural forms of sterol in membranes of living cells. *J Biol Chem*. 2003;278:6384–6403.
46. Kohut P, Wüstner D, Hronska L, Kuchler K, Hapala I, Valachovic M. The role of ABC proteins Aus1p and Pdr11p in the uptake of external sterols in yeast: dehydroergosterol fluorescence study. *Biochem Biophys Res Commun*. 2011;404:233–238.
47. Georgiev AG, Sullivan DP, Kersting MC, Dittman JS, Beh CT, Menon AK. Osh proteins regulate membrane sterol organization but are not required for sterol movement between the ER and PM. *Traffic*. 2011;12:1341–1355.
48. Wüstner D, Mondal M, Tabas I, Maxfield FR. Direct observation of rapid internalization and intracellular transport of sterol by macrophage foam cells. *Traffic*. 2005;6:396–412.
49. Hölttä-Vuori M, Uronen RL, Repakova J, et al. BODIPY-cholesterol: a new tool to visualize sterol trafficking in living cells and organisms. *Traffic*. 2008;9:1839–1849.
50. Liu J, Chang CC, Westover EJ, Covey DF, Chang TY. Investigating the allosterism of acyl-CoA:cholesterol acyltransferase (ACAT) by using various sterols: in vitro and intact cell studies. *Biochem J*. 2005;391:389–397.
51. Mesmin B, Pipalia NH, Lund FW, et al. STARD4 abundance regulates sterol transport and sensing. *Mol Biol Cell*. 2011;22:4004–4015.
52. Pourmousa M, Róg T, Mikkeli R, et al. Dehydroergosterol as an analogue for cholesterol: why it mimics cholesterol so well or does it? *J Phys Chem*. 2014;118:7345–7357.
53. Scheidt HA, Müller P, Herrmann A, Huster D. The potential of fluorescent and spin-labeled steroid analogs to mimic natural cholesterol. *J Biol Chem*. 2003;278:45563–45569.
54. Henriksen J, Rowat AC, Brief E, et al. Universal behavior of membranes with sterols. *Biophys J*. 2006;90:1639–1649.

55. Arora A, Raghuraman H, Chattopadhyay A. Influence of cholesterol and ergosterol on membrane dynamics: a fluorescence approach. *Biochem Biophys Res Commun*. 2004;318:920–926.
56. Wüstner D, Herrmann A, Hao M, Maxfield FR. Rapid nonvesicular transport of sterol between the plasma membrane domains of polarized hepatic cells. *J Biol Chem*. 2002;277:30325–30336.
57. Smutzer G, Crawford BF, Yeagle PL. Physical properties of the fluorescent sterol probe dehydroergosterol. *Biochim Biophys Acta*. 1986;862:361–371.
58. Loura LM, Prieto M. Dehydroergosterol structural organization in aqueous medium and in a model system of membranes. *Biophys J*. 1997;72:2226–2236.
59. Harris JS, Epps DE, Davio SR, Kezdy FJ. Evidence for transbilayer, tail-to-tail cholesterol dimers in dipalmitoylglycerophosphocholine liposomes. *Biochemistry*. 1995;34:3851–3857.
60. Wüstner D. Fluorescent sterols as tools in membrane biophysics and cell biology. *Chem Phys Lipids*. 2007;146:1–25.
61. Frolov A, Petrescu A, Atshaves BP, et al. High density lipoprotein-mediated cholesterol uptake and targeting to lipid droplets in intact L-cell fibroblasts. *J Biol Chem*. 2000;275:12769–12780.
62. Wüstner D, Brewer JR, Bagatolli LA, Sage D. Potential of ultraviolet widefield imaging and multiphoton microscopy for analysis of dehydroergosterol in cellular membranes. *Microsc Res Tech*. 2011;74:92–108.
63. Wüstner D, Landt Larsen A, Færgeman NJ, Brewer JR, Sage D. Selective visualization of fluorescent sterols in *Caenorhabditis elegans* by bleach-rate based image segmentation. *Traffic*. 2010;11:440–454.
64. Zipfel WR, Williams RM, Webb WW. Nonlinear magic: multiphoton microscopy in the biosciences. *Nat Biotechnol*. 2003;21:1369–1377.
65. Luisier F, Vonesch C, Blu T, Unser M. Fast interscale wavelet denoising of Poisson-corrupted images. *Signal Processing*. 2010;90:415–427.
66. Gerstbrein B, Stamatas G, Kollias N, Driscoll M. In vivo spectrofluorimetry reveals endogenous biomarkers that report healthspan and dietary restriction in *Caenorhabditis elegans*. *Aging Cell*. 2005;4:127–137.
67. Wüstner D, Sage D. Multicolor bleach-rate imaging enlightens in vivo sterol transport. *Commun Integr Biol*. 2010;3:1–4.
68. Albro PW, Bilski P, Corbett JT, Schroeder JL, Chignell CF. Photochemical reactions and phototoxicity of sterols: novel self-perpetuating mechanisms for lipid photoxidation. *Photochem Photobiol*. 1997;66:316–325.
69. Windaus A, Deppe M, Roosen-Runge C. The pyro-vitamin D and its dehydroderivative. *Liebigs Ann Chem*. 1939;537:1–10.
70. Antonucci R, Bernstein S, Giancola D, Sax KJ. Delta-5, 7-steroids.7. The conversion of delta-5, 7-steroidal to delta-5, 7,9-steroidal hormones. *J Org Chem*. 1951; 16:1159-1164.
71. Fischer RT, Stephenson FA, Shafiee A, Schroeder F. Delta-5,7,9(11)-cholestatrien-3beta-Ol—a fluorescent cholesterol analog. *Chem Phys Lipids*. 1984; 36:1–14.
72. Wüstner D, Færgeman NJ. Spatiotemporal analysis of endocytosis and membrane distribution of fluorescent sterols in living cells. *Histochem Cell Biol*. 2008; 130:891–908.
73. Mondal M, Mesmin B, Mukherjee S, Maxfield FR. Sterols are mainly in the cytoplasmic leaflet of the plasma membrane and the endocytic recycling compartment in CHO cells. *Mol Biol Cell*. 2009;20:581–588.
74. Garvik O, Benediktson P, Simonsen AC, Ipsen JH, Wüstner D. The fluorescent cholesterol analog dehydroergosterol induces liquid-ordered domains in model membranes. *Chem Phys Lipids*. 2009;159:114–118.
75. Schroeder F, Dempsey ME, Fischer RT. Sterol and squalene carrier protein interactions with fluorescent delta-5,7,9(11)-cholestatrien-3-beta-Ol. *J Biol Chem*. 1985;260:2904–2911.
76. Schroeder F, Nemecz G, Gratton E, Barenholz Y, Thompson TE. Fluorescence properties of cholestatrienol in phosphatidylcholine bilayer vesicles. *Biophys Chem*. 1988;32:57–72.
77. Hyslop PA, Morel B, Sauerheber RD. Organization and interaction of cholesterol and phosphatidylcholine in model bilayer membranes. *Biochemistry*. 1990; 29:1025–1038.
78. Yeagle PL, Albert AD, Boesze-Battaglia K, Young J, Frye J. Cholesterol dynamics in membranes. *Biophys J*. 1990;57:413–424.
79. Robalo JR, do Canto AM, Carvalho AJ, Ramalho JP, Loura LM. Behavior of fluorescent cholesterol analogues dehydroergosterol and cholestatrienol in lipid bilayers: a molecular dynamics study. *J Phys Chem B*. 2013;117:5806–5819.
80. Näbo LJ, List NH, Witzke S, Wüstner D, Khandelia H, Kongsted J. Design of new fluorescent cholesterol and ergosterol analogs: insights from theory. *Biochim Biophys Acta*. 2015;1848:2188–2199.
81. Yeagle PL, Bensen J, Boni L, Hui SW. Molecular packing of cholesterol in phospholipid vesicles as probed by dehydroergosterol. *Biochim Biophys Acta*. 1982;692: 139–146.
82. Chong PL, Thompson TE. Depolarization of dehydroergosterol in phospholipid bilayers. *Biochim Biophys Acta*. 1986;863:53–62.
83. Chong PL. Evidence for regular distribution of sterols in liquid crystalline phosphatidylcholine bilayers. *Proc Natl Acad Sci U S A*. 1994;91:10069–10073.
84. Ipsen JH, Karlstrom G, Mouritsen OG, Wennerstrom H, Zuckermann MJ. Phase equilibria in the phosphatidylcholine-cholesterol system. *Biochim Biophys Acta*. 1987;905:162–172.
85. Veatch SL, Keller SL. Separation of liquid phases in giant vesicles of ternary mixtures of phospholipids and cholesterol. *Biophys J*. 2003;85:3074–3083.
86. Baumgart T, Hunt G, Farkas ER, Webb WW, Feigenson GW. Fluorescence probe partitioning between Lo/Ld phases in lipid membranes. *Biochim Biophys Acta*. 2007;1768:2182–2194.
87. Sezgin E, Levental I, Grzybek M, et al. Partitioning, diffusion, and ligand binding of raft lipid analogs in model and cellular plasma membranes. *Biochim Biophys Acta*. 2012;1818:1777–1784.
88. Wüstner D, Solanko LM, Sokol E, et al. Quantitative assessment of sterol traffic in living cells by dual labeling with dehydroergosterol and BODIPY-cholesterol. *Chem Phys Lipids*. 2011;164:221–235.
89. Loura LMS, Fedorov A, Prieto M. Exclusion of a cholesterol analog from the cholesterol-rich phase in model membranes. *Biochim Biophys Acta*. 2001;1511:236–243.
90. Loura LMS, Fedorov A, Prieto M. Partition of membrane probes in a gel/fluid two-component lipid system: a fluorescence resonance energy transfer study. *Biochim Biophys Acta*. 2000;1467:101–112.
91. Wüstner D. Plasma membrane sterol distribution resembles the surface topography of living cells. *Mol Biol Cell*. 2007;18:211–228.
92. Wüstner D. Free-cholesterol loading does not trigger phase separation of the fluorescent sterol dehydroergosterol in the plasma membrane of macrophages. *Chem Phys Lipids*. 2008;154:129–136.
93. Anderton CR, Lou K, Weber PK, Hutcheon ID, Kraft ML. Correlated AFM and NanoSIMS imaging to probe cholesterol-induced changes in phase behavior and non-ideal mixing in ternary lipid membranes. *Biochim Biophys Acta*. 2011; 1808:307–315.
94. Frisz JF, Klitzing HA, Lou K, et al. Sphingolipid domains in the plasma membranes of fibroblasts are not enriched with cholesterol. *J Biol Chem*. 2013;288: 16855–16861.
95. Mayor S, Maxfield FR. Insolubility and redistribution of GPI-anchored proteins at the cell surface after detergent treatment. *Mol Biol Cell*. 1995;6:929–944.
96. Hao M, Mukherjee S, Maxfield FR. Cholesterol depletion induces large scale domain segregation in living cell membranes. *Proc Natl Acad Sci U S A*. 2001;98: 13072–13077.
97. Sezgin E, Betul Can F, Schneider F, et al. A comparative study on fluorescent cholesterol analogs as versatile cellular reporters. *J Lipid Res*. 2016;57(2):299–309.
98. Sezgin E, Kaiser HJ, Baumgart T, Schwille P, Simons K, Levental I. Elucidating membrane structure and protein behavior using giant plasma membrane vesicles. *Nat Protoc*. 2012;7:1042–1051.
99. Pagler TA, Wang M, Mondal M, et al. Deletion of ABCA1 and ABCG1 impairs macrophage migration because of increased Rac1 signaling. *Circ Res*. 2011;108: 194–200.
100. Wüstner D, Modzel M, Lund FW, Lomholt MA. Imaging approaches for analysis of cholesterol distribution and dynamics in the plasma membrane. *Chem Phys Lipids*. 2016. http://dx.doi.org/10.1016/j.chemphyslip.2016.03.003
101. Hartwig Petersen N, Færgeman NJ, Yu L, Wüstner D. Kinetic imaging of NPC1L1 and sterol trafficking between plasma membrane and recycling endosomes in hepatoma cells. *J Lipid Res*. 2008;49:2023–2037.
102. Xu Z, Farver W, Kodukula S, Storch J. Regulation of sterol transport between membranes and NPC2. *Biochemistry*. 2008;47:11134–11143.
103. Ngo M, Ridgway ND. Oxysterol binding protein-related protein 9 (ORP9) is a cholesterol transfer protein that regulates Golgi structure and function. *Mol Biol Cell*. 2009;20:1388–1399.
104. Iaea DB, Gale SE, Bielska AA, et al. A novel intrinsically fluorescent probe for study of uptake and trafficking of 25-hydroxycholesterol. *J Lipid Res*. 2015; 56(12):2408–2419.
105. Patel KM, Sklar LA, Currie R, Pownall HJ, Morrisett JD, Sparrow JT. Synthesis of saturated, unsaturated, spin-labeled, and fluorescent cholesteryl esters—acylation of cholesterol using fatty-acid anhydride and 4-pyrrolidinopyridine. *Lipids*. 1979;14:816–818.
106. Pattnaik NM, Montes A, Hughes LB, Zilversmit DB. Cholesteryl ester exchange protein in human-plasma isolation and characterization. *Biochim Biophys Acta*. 1978;530:428–438.
107. Krieger M, Brown MS, Faust JR, Goldstein JL. Replacement of endogenous cholesteryl esters of low-density lipoprotein with exogenous cholesteryl linoleate—reconstitution of a biologically-active lipoprotein particle. *J Biol Chem*. 1978;253:4093–4101.
108. Smith RJ, Green C. Fluorescence studies of protein-sterol relationships in human plasma lipoproteins. *Biochem J*. 1974;137:413–415.
109. Sklar LA, Craig IF, Pownall HJ. Induced circular-dichroism of incorporated fluorescent cholesteryl esters and polar lipids as a probe of human-serum low-density lipoprotein structure and melting. *J Biol Chem*. 1981;256:4286–4292.
110. Schroeder F, Goh EH, Heimberg M. Regulation of the surface physical properties of the very low density lipoprotein. *J Biol Chem*. 1979;254:2456–2463.
111. Sklar LA, Mantulin WW, Ponwall HJ. Fluorescent cholesteryl esters in the core of low density lipoprotein. *Biochem Biophys Res Commun*. 1982;105:674–680.

112. Riley JP. The seed fat of parinarium laurinum.1. Component acids of the seed fat. *J Chem Soc*. 1950:12–18.
113. Lee SJ, Gray KC, Paek JS, Burke MD. Simple, efficient, and modular syntheses of polyene natural products via iterative cross-coupling. *J Am Chem Soc*. 2008;130: 466–468.
114. Sklar LA, Hudson BS, Simoni RD. Conjugated polyene fatty-acids as membrane probes—preliminary characterization. *Proc Natl Acad Sci U S A*. 1975;72: 1649–1653.
115. Sklar LA, Hudson BS, Simoni RD. Conjugated polyene fatty-acids as fluorescent-probes—synthetic phospholipid membrane studies. *Biochemistry*. 1977;16: 819–828.
116. Benyashar V, Barenholz Y. Characterization of the core and surface of human plasma-lipoproteins—a study based on the use of 5 fluorophores. *Chem Phys Lipids*. 1991;60:1–14.
117. Sibarita JB. Deconvolution microscopy. *Adv Biochem Eng Biotechnol*. 2005;95: 201–243.
118. Heintzmann R. Estimating missing information by maximum likelihood deconvolution. *Micron*. 2007;38:136–144.
119. Kirshner H, Aguet F, Sage D, Unser M. 3-D PSF fitting for fluorescence microscopy: implementation and localization application. *J Microsc*. 2013;249: 13–25.
120. Bertero M, Boccacci P. Super-resolution in computational imaging. *Micron*. 2003;34:265–273.
121. Stelzer EHK. Contrast, resolution, pixelation, dynamic range and signal-to-noise ratio: fundamental limits to resolution in fluorescence light microscopy. *J Microsc*. 1998;189:15–24.
122. Wustner D, Christensen T, Solanko LM, Sage D. Photobleaching kinetics and time-integrated emission of fluorescent probes in cellular membranes. *Molecules*. 2014;19:11096–11130.
123. Marks DL, Bittman R, Pagano RE. Use of Bodipy-labeled sphingolipid and cholesterol analogs to examine membrane microdomains in cells. *Histochem Cell Biol*. 2008;130:819–832.
124. Li ZG, Mintzer E, Bittman R. First synthesis of free cholesterol-BODIPY conjugates. *J Org Chem*. 2006;71:1718–1721.
125. Wüstner D, Lund FW, Röhrl C, Stangl H. Potential of BODIPY-cholesterol for analysis of cholesterol transport and diffusion in living cells. *Chem Phys Lipids*. 2016;194:12–28.
126. Liu Z, Thacker SG, Fernandez-Castillejo S, Neufeld EB, Remaley AT, Bittman R. Synthesis of cholesterol analogues bearing BODIPY fluorophores by Suzuki or Liebeskind-Srogl cross-coupling and evaluation of their potential for visualization of cholesterol pools. *Chembiochem*. 2014;15:2087–2096.
127. Shaw JE, Epand RF, Epand RM, Li Z, Bittman R, Yip CM. Correlated fluorescence-atomic force microscopy of membrane domains: structure of fluorescence probes determines lipid localization. *Biophys J*. 2006;90:2170–2178.
128. Solanko LM, Honigmann A, Midtiby HS, et al. Membrane orientation and lateral diffusion of BODIPY-cholesterol as a function of probe structure. *Biophys J*. 2013;105:2082–2092.
129. Lund FW, Lomholt MA, Solanko LM, Bittman R, Wüstner D. Two-photon time-lapse microscopy of BODIPY-cholesterol reveals anomalous sterol diffusion in Chinese hamster ovary cells. *BMC Biophys*. 2012;5:20.
130. Hiramoto-Yamaki N, Tanaka KA, Suzuki KG, et al. Ultrafast diffusion of a fluorescent cholesterol analog in compartmentalized plasma membranes. *Traffic*. 2014;15(6):583–612.
131. Honigmann A, Mueller V, Ta H, et al. Scanning STED-FCS reveals spatiotemporal heterogeneity of lipid interaction in the plasma membrane of living cells. *Nat Commun*. 2014;5:5412.
132. Sevcsik E, Brameshuber M, Folser M, Weghuber J, Honigmann A, Schutz GJ. GPI-anchored proteins do not reside in ordered domains in the live cell plasma membrane. *Nat Commun*. 2015;6:6969.
133. Lee HJ, Zhang W, Zhang D, et al. Assessing cholesterol storage in live cells and *C. elegans* by stimulated Raman scattering imaging of phenyl-Diyne cholesterol. *Sci Rep*. 2015;5:7930.
134. Listenberger LL, Brown DA. Fluorescent detection of lipid droplets and associated proteins. *Curr Protoc Cell Biol*. 2007:24. doi: 10.1002/0471143030.cb2402s35.
135. Milles S, Meyer T, Scheidt HA, et al. Organization of fluorescent cholesterol analogs in lipid bilayers—lessons from cyclodextrin extraction. *Biochim Biophys Acta*. 2013;1828:1822–1828.
136. Kanerva K, Uronen RL, Blom T, et al. LDL cholesterol recycles to the plasma membrane via a Rab8a-Myosin5b-actin-dependent membrane transport route. *Dev Cell*. 2013;27:249–262.
137. Krieger M. Reconstitution of the hydrophobic core of low-density-lipoprotein. *Methods Enzymol*. 1986;128:608–613.
138. Röhrl C, Meisslitzer-Ruppitsch C, Bittman R, et al. Combined light and electron microscopy using diaminobenzidine photooxidation to monitor trafficking of lipids derived from lipoprotein particles. *Curr Pharm Biotechnol*. 2012;13: 331–340.
139. Silver DL, Wang N, Xiao X, Tall AR. High density lipoprotein (HDL) particle uptake mediated by scavenger receptor class B type 1 results in selective sorting of HDL cholesterol from protein and polarized cholesterol secretion. *J Biol Chem*. 2001;276:25287–25293.
140. Wüstner D. Mathematical analysis of hepatic high density lipoprotein transport based on quantitative imaging data. *J Biol Chem*. 2005;280:6766–6779.
141. Ikonen E, Blom T. Lipoprotein-mediated delivery of BODIPY-labeled sterol and sphingolipid analogs reveals lipid transport mechanisms in mammalian cells. *Chem Phys Lipids*. 2016;194:29–36.
142. Bernik DL, Negri RM. Local polarity at the polar head level of lipid vesicles using dansyl fluorescent probes. *J Colloid Interface Sci*. 1998;203:97–105.
143. Wiegand V, Chang TY, Strauss JF III, Fahrenholz F, Gimpl G. Transport of plasma membrane-derived cholesterol and the function of Niemann-Pick C1 protein. *FASEB J*. 2003;17:782–784.
144. Huang H, McIntosh AL, Atshaves BP, Ohno-Iwashita Y, Kier AB, Schroeder F. Use of dansyl-cholestanol as a probe of cholesterol behavior in membranes of living cells. *J Lipid Res*. 2010;51:1157–1172.
145. Haberland ME, Reynolds JA. Self-association of cholesterol in aqueous solution. *Proc Natl Acad Sci U S A*. 1973;70:2313–2318.
146. Stubbs CD, Meech SR, Lee AG, Phillips D. Solvent relaxation in lipid bilayers with dansyl probes. *Biochim Biophys Acta*. 1985;815:351–360.
147. Shrivastava S, Haldar S, Gimpl G, Chattopadhyay A. Orientation and dynamics of a novel fluorescent cholesterol analogue in membranes of varying phase. *J Phys Chem B*. 2009;113:4475–4481.
148. Chattopadhyay A, London E. Parallax method for direct measurement of membrane penetration depth utilizing fluorescence quenching by spin-labeled phospholipids. *Biochemistry*. 1987;26:39–45.
149. Leonard A, Escrive C, Laguerre M, et al. Location of cholesterol in DMPC membranes. A comparative study by neutron diffraction and molecular mechanics simulation. *Langmuir*. 2001;17:2019–2030.
150. Petrescu AD, Vespa A, Huang H, McIntosh AL, Schroeder F, Kier AB. Fluorescent sterols monitor cell penetrating peptide Pep-1 mediated uptake and intracellular targeting of cargo protein in living cells. *Biochim Biophys Acta*. 2009;1788: 425–441.
151. Wrenn SP, Kaler EW, Lee SP. A fluorescence energy transfer study of lecithin-cholesterol vesicles in the presence of phospholipase C. *J Lipid Res*. 1999;40: 1483–1494.
152. Wrenn SP, Gudheti M, Veleva AN, Kaler EW, Lee SP. Characterization of model bile using fluorescence energy transfer from dehydroergosterol to dansylated lecithin. *J Lipid Res*. 2001;42:923–934.
153. John K, Kubelt J, Muller P, Wustner D, Herrmann A. Rapid transbilayer movement of the fluorescent sterol dehydroergosterol in lipid membranes. *Biophys J*. 2002;83:1525–1534.
154. Benson DM, Bryan J, Plant AL, Gotto AMJ, Smith LC. Digital imaging fluorescence microscopy: spatial heterogeneity of photobleaching rate constants in individual cells. *J Cell Biol*. 1985;100:1309–1323.
155. Craig IF, Via DP, Mantulin WW, Pownall HJ, Gotto AM Jr, Smith LC. Low density lipoproteins reconstituted with steroids containing the nitrobenzoxadiazole fluorophore. *J Lipid Res*. 1981;22:687–696.
156. Gimpl G, Gehrig-Burger K. Cholesterol reporter molecules. *Biosci Rep*. 2007; 27:335–358.
157. Reiner S, Micolod D, Schneiter R. *Saccharomyces cerevisiae*, a model to study sterol uptake and transport in eukaryotes. *Biochem Soc Trans*. 2005;33: 1186–1188.
158. Marek M, Silvestro D, Fredslund MD, Andersen TG, Pomorski TG. Serum albumin promotes ATP-binding cassette transporter-dependent sterol uptake in yeast. *FEMS Yeast Res*. 2014;14:1223–1233.
159. Ishii H, Shimanouchi T, Umakoshi H, Walde P, Kuboi R. Analysis of the 22-NBD-cholesterol transfer between liposome membranes and its relation to the intermembrane exchange of 25-hydroxycholesterol. *Colloids Surf B Biointerfaces*. 2010;77:117–121.
160. Bar LK, Chong PL, Barenholz Y, Thompson TE. Spontaneous transfer between phospholipid bilayers of dehydroergosterol, a fluorescent cholesterol analog. *Biochim Biophys Acta*. 1989;983:109–112.
161. Bar LK, Barenholz Y, Thompson TE. Fraction of cholesterol undergoing spontaneous exchange between small unilamellar phosphatidylcholine vesicles. *Biochemistry*. 1986;25:6701–6705.
162. Ostašov P, Sýkora J, Brejchová J, Olžyńska A, Hof M, Svoboda P. FLIM studies of 22- and 25-NBD-cholesterol in living HEK293 cells: plasma membrane change induced by cholesterol depletion. *Chem Phys Lipids*. 2013;167–168: 62–69.
163. Mukherjee S, Zha X, Tabas I, Maxfield FR. Cholesterol distribution in living cells: fluorescence imaging using dehydroergosterol as a fluorescent cholesterol analog. *Biophys J*. 1998;75:1915–1925.
164. Faletrov YV, Bialevich KI, Edimecheva IP, et al. 22-NBD-cholesterol as a novel fluorescent substrate for cholesterol-converting oxidoreductases. *J Steroid Biochem Mol Biol*. 2013;134:59–66.

165. Faletrov YV, Frolova NS, Hlushko HV, et al. Evaluation of the fluorescent probes Nile Red and 25-NBD-cholesterol as substrates for steroid-converting oxidoreductases using pure enzymes and microorganisms. *FEBS J*. 2013;280:3109–3119.
166. Kheirolomoom A, Ferrara KW. Cholesterol transport from liposomal delivery vehicles. *Biomaterials*. 2007;28:4311–4320.
167. Sparrow CP, Patel S, Baffic J, et al. A fluorescent cholesterol analog traces cholesterol absorption in hamsters and is esterified in vivo and in vitro. *J Lipid Res*. 1999;40:1747–1757.
168. Lada AT, Davis M, Kent C, et al. Identification of ACAT1- and ACAT2-specific inhibitors using a novel, cell-based fluorescence assay: individual ACAT uniqueness. *J Lipid Res*. 2004;45:378–386.
169. Reiner S, Micolod D, Zellnig G, Schneiter R. A genomewide screen reveals a role of mitochondria in anaerobic uptake of sterols in yeast. *Mol Biol Cell*. 2005; 17:90–103.
170. Lusa S, Jauhiainen M, Metso J, Somerharju P, Ehnholm C. The mechanism of human plasma phospholipid transfer protein-induced enlargement of high-density lipoprotein particles: evidence for particle fusion. *Biochem J*. 1996;313(pt 1): 275–282.
171. Lusa S, Tanhuanpaa K, Ezra T, Somerharju P. Direct observation of lipoprotein cholesterol ester degradation in lysosomes. *Biochem J*. 1998;332(pt 2):451–457.
172. Le Guyader L, Le Roux C, Mazères S, et al. Changes of the membrane lipid organization characterized by means of a new cholesterol-pyrene probe. *Biophys J*. 2007;93:4462–4473.
173. Repáková J, Holopainen JM, Karttunen M, Vattulainen I. Influence of pyrene-labeling on fluid lipid membranes. *J Phys Chem B*. 2006;110:15403–15410.
174. Gaibelet G, Terce F, Bertrand-Michel J, et al. 21-Methylpyrenyl-cholesterol stably and specifically associates with lipoprotein peripheral hemi-membrane: a new labelling tool. *Biochem Biophys Res Commun*. 2013;440:533–538.
175. Gaibelet G, Allart S, Terce F, et al. Specific cellular incorporation of a pyrene-labelled cholesterol: lipoprotein-mediated delivery toward ordered intracellular membranes. *PLoS One*. 2015;10:e0121563.
176. Kolb HC, Sharpless KB. The growing impact of click chemistry on drug discovery. *Drug Discov Today*. 2003;8:1128–1137.
177. Gaebler A, Milan R, Straub L, Hoelper D, Kuerschner L, Thiele C. Alkyne lipids as substrates for click chemistry-based in vitro enzymatic assays. *J Lipid Res*. 2013;54:2282–2290.
178. Thiele C, Papan C, Hoelper D, et al. Tracing fatty acid metabolism by click chemistry. *ACS Chem Biol*. 2012;7:2004–2011.
179. Hofmann K, Thiele C, Schott HF, et al. A novel alkyne cholesterol to trace cellular cholesterol metabolism and localization. *J Lipid Res*. 2014;55:583–591.
180. Peyrot SM, Nachtergaele S, Luchetti G, et al. Tracking the subcellular fate of 20(S)-hydroxycholesterol with click chemistry reveals a transport pathway to the Golgi. *J Biol Chem*. 2014;289:11095–11110.
181. Yamakoshi H, Dodo K, Palonpon A, et al. Alkyne-tag Raman imaging for visualization of mobile small molecules in live cells. *J Am Chem Soc*. 2012;134: 20681–20689.
182. Scheidt HA, Meyer T, Nikolaus J, et al. Cholesterol's aliphatic side chain modulates membrane properties. *Angew Chem Int Ed Engl*. 2013;52:12848–12851.
183. Meyer T, Baek DJ, Bittman R, et al. Membrane properties of cholesterol analogs with an unbranched aliphatic side chain. *Chem Phys Lipids*. 2014;184:1–6.
184. Chien CH, Chen WW, Wu JT, Chang TC. Label-free imaging of *Drosophila* in vivo by coherent anti-Stokes Raman scattering and two-photon excitation autofluorescence microscopy. *J Biomed Opt*. 2011;16:016012.
185. Jao CY, Nedelcu D, Lopez LV, Samarakoon TN, Welti R, Salic A. Bioorthogonal probes for imaging sterols in cells. *Chembiochem*. 2015;16:611–617.
186. Sletten EM, Bertozzi CR. From mechanism to mouse: a tale of two bioorthogonal reactions. *Acc Chem Res*. 2011;44:666–676.
187. Baskin JM, Prescher JA, Laughlin ST, et al. Copper-free click chemistry for dynamic in vivo imaging. *Proc Natl Acad Sci U S A*. 2007;104:16793–16797.
188. Wüstner D, Lund FW, Solanko LM. Quantitative fluorescence studies of intracellular sterol transport and distribution. In: Mely Y, Duportail G, eds. *Springer Series in Fluorescence. Properties and Functions of Biological Membranes Investigated by Fluorescence Methods*. Springer Press, Berlin Heidelberg; 2012:185–213.